Sustainable Energy & Fuels

ROYAL SOCIETY OF CHEMISTRY

PERSPECTIVE

View Article Online
View Journal | View Issue

Cite this: *Sustainable Energy Fuels*, 2023, 7, 5445

Electrochemical CO_2 conversion technologies: state-of-the-art and future perspectives†

Remko J. Detz, *[a] Claire J. Ferchaud,[b] Arie J. Kalkman,[c] Jasmin Kemper,[d] Carlos Sánchez-Martínez,[c] Marija Saric[b] and Manoj V. Shinde[b]

Electrochemical reduction of CO_2 to produce chemicals or fuels may contribute to the zero-emission goal of the chemical industry. Here, we report the state-of-the-art and future perspective of electrochemical CO_2 conversion processes to produce CO, syngas, formic acid and ethylene. We selected and explored six routes: low-temperature CO production, low-temperature formic acid production, low-temperature ethylene production, high-temperature CO production, high-temperature syngas production, and a tandem approach to produce ethylene. For these routes, we describe the current level of development, performance indicators, and costs. The state-of-the-art of the chlor-alkali process is included as an example of a commercially applied electrochemical process. We calculate the economic performance of the various pathways in terms of levelized production costs and we use a learning curve method to project costs up to 2050. The greenhouse gas performance for all routes is determined and compared to the current reference of production from fossil-based resources. We conclude that high-temperature solid-oxide electrolysis to produce CO and syngas is the most developed and closest to reaching break-even levelized production cost in comparison to the fossil reference. Low-temperature electrolysis processes are at a lower technology readiness level and still need a substantial reduction in investment costs and improvements in process efficiency to achieve break-even with incumbent technology. The most promising of the low-temperature processes is formic acid production. Electrochemical production of formic acid, CO, and syngas results or can soon result in substantial GHG savings compared to their fossil-based alternatives. The extent to which savings can be achieved depends merely on the carbon intensity of the local power grid, or more generally, the supplied electricity. Electrochemical CO_2 conversion to produce ethylene would require a very low emission factor of electricity (<50 g_{CO_2} per kW h) to be competitive with current production methods and is therefore not likely to contribute significantly to the zero-emission goal of the petrochemical industry in the foreseeable future. Research gaps are identified at various levels: improvement of the performance of the various components, such as catalysts and electrodes, and of purification of feedstock and product streams. Pilot and demonstration projects of the entire value chain from the CO_2 stream to the final product are needed to more accurately determine the performance, total investment costs, and operating and maintenance costs in an industrial environment.

Received 15th June 2023
Accepted 11th September 2023

DOI: 10.1039/d3se00775h

rsc.li/sustainable-energy

1 Introduction

The use of fossil resources provides the world with highly concentrated forms of energy, but additionally with an abundance of carbon. Due to fuel combustion and waste incineration, a substantial share of this carbon is emitted to the atmosphere as carbon dioxide (CO_2). Next to these undesirable CO_2 emissions, many materials that are used in society, for example, bitumen, lubricants, plastics, and solvents, contain carbon as the main element. A vital climate change mitigation option encompasses the reduction of greenhouse gas (GHG) emissions of which fossil CO_2 emissions account for roughly 70%.[1] Various technologies to provide renewable energy, such as solar photovoltaics and wind turbines, are currently being

[a]*Energy Transition Studies (ETS), Netherlands Organization for Applied Scientific Research (TNO), Radarweg 60, 1043 NT Amsterdam, The Netherlands. E-mail: remko.detz@tno.nl*

[b]*Sustainable Technologies for Industrial Processes (STIP), Netherlands Organization for Applied Scientific Research (TNO), P.O. Box 1, 1755 ZG Petten, The Netherlands*

[c]*Sustainable Process and Energy Systems (SPES), Netherlands Organization for Applied Scientific Research (TNO), P.O. Box 6012, 2600 JA Delft, The Netherlands*

[d]*IEA Greenhouse Gas R&D Programme, Pure Offices, Cheltenham Office Park, Hatherley Lane, Cheltenham, GLOS, GL51 6SH, UK*

† Electronic supplementary information (ESI) available. See DOI: https://doi.org/10.1039/d3se00775h

deployed to avoid and replace the use of fossil fuels. Abandoning the use of fossil resources will eventually also reduce the availability of carbon as a feedstock to produce fuels, chemicals, building materials, and polymers. To find alternatives to fossil carbon, the chemical industry is already exploring various pathways to use circular flows of carbon, originating from either biogenic or atmospheric sources, or waste streams.[2]

Carbon capture and utilization (CCU) technologies show promise for providing valuable, cost-competitive products to the economy while simultaneously mitigating CO_2 emissions and climate change. Increased electrification and the increase of carbon-free, intermittent electricity have attracted global interest towards flexible CCU systems driven by electrical power. Electrochemical systems use electrons to reduce, for instance, CO_2 into a multitude of products. This variety of products mirrors the diversity of electrochemical systems under development. For example, proton exchange membrane (PEM) electrolysers function under (near) ambient conditions, while solid-oxide systems can operate at temperatures above 700 °C. Unfortunately, existing CO_2 conversion processes are energy-intensive and expensive. R&D efforts typically focus on improving the energy efficiency and selectivity of laboratory-scale demonstrations. More information is needed to understand the technical and economic hurdles that unique reactor systems may face when scaling from laboratory and bench scale projects to demonstration and pilot scale applications.

In this study, we review the use of CO_2 as feedstock, also known as carbon capture and utilization (CCU) routes, to produce carbon-based chemicals, with a focus on carbon monoxide (CO), syngas (CO/H_2), formic acid (FA), and ethylene (C_2H_4). Different sources of CO_2 are available, such as biomass, atmosphere, ocean, or fossil resources. The origin of the CO_2 feedstock is not part of this assessment but has important implications for, for instance, the costs, energy demand, accessibility, scale, societal acceptance, and sustainability of the route.[3] CCU may have substantial market opportunities if it can replace part of the fossil fuels and the chemical industry and this prospect encourages several stakeholders to investigate different approaches to convert CO_2 into products.[3–5] Many routes at various stages of technological maturity are being developed. The different approaches, such as biochemical synthesis,[6] carbonation, electroconversion, photoreduction,[7,8] and thermocatalysis,[9] are schematically depicted in Fig. 1.

We here examine six electroconversion routes that apply electricity as an energy carrier to directly convert CO_2 into products by electrochemical means. Such an approach has several advantages in that it can: (1) accelerate the uptake of renewable electricity supply thanks to increased demand; (2) reduce the reliance of industry on fossil fuels by enhancing industrial electrification; (3) result in more efficient (ideally) single-step conversion processes that can lead to pure products and simplify purification steps.

In Chapter 2, we discuss the state-of-the-art in terms of the development stage and performance metrics of direct electrochemical CO_2 conversion approaches. Several processes and products are thoroughly studied at the laboratory scale,[10–16] but only a few are more advanced in their development stage. We have selected six routes, mainly based on the technology readiness level (TRL > 4: routes 1, 2, 4, and 5) and two potentially interesting approaches to produce ethylene (TRL 3–4: routes 3 and 6), for further techno-economic assessment (Table 1).

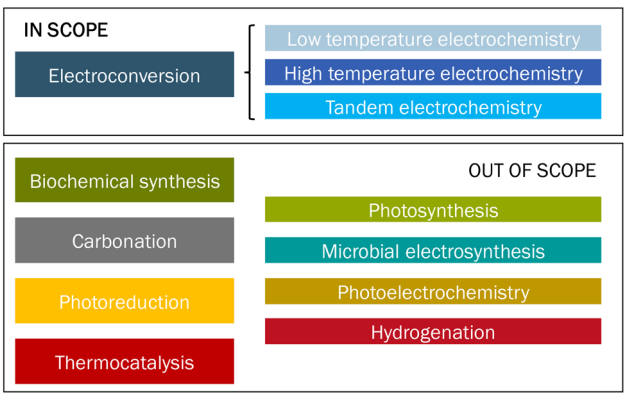

Fig. 1 Overview of different approaches to convert CO_2 into products. The category 'Tandem electrochemistry' refers to a combination of high- and low-temperature electroconversion of CO_2 to products.

Table 1 Scope overview with electrochemical CO_2 conversion technologies and products. Green ticks (✓) indicate routes that are relatively advanced (TRL > 4) and are within the scope of this study. Beaker symbols (🧪) indicate processes that are currently at a relatively early development stage (TRL < 4) and are outside the scope of this study, except for two processes to produce C_2H_4. LT = low temperature; HT = high temperature; SOEC = solid oxide electrolysis cell; MCEC = molten carbonate electrolysis cell; FA = formic acid; MeOH = methanol; OxA = oxalic acid; EtOH = ethanol; PrOH = *n*-propanol

Product type		Gaseous single carbon			Liquid single carbon			Gaseous and liquid multi-carbon			
Technology line		CO	CO/H_2	CH_4	FA	MeOH	CH_2O	C_2H_4	OxA	EtOH	PrOH
LT		✓	🧪	🧪	✓	🧪	🧪	✓ 🧪	🧪	🧪	🧪
HT	SOEC	✓	✓								
	MCEC	🧪	🧪								
Tandem HT/LT								✓			

For these routes, we determine and discuss the current costs and apply learning curve analysis to project costs up to 2050 (Chapter 3). At that time, the technology needs to be competitive at an industrial scale in order to play a meaningful role in the energy transition. To contextualize the analysis of these CCU electrochemical conversion processes, the state-of-the-art of chlor-alkali production as an existing, industrial-scale electrochemical process has been evaluated as well. The chlor-alkali industry has demonstrated that it is feasible to build and operate industrial scale electrochemical installations. These installations will likely serve as a prime example for future electrochemical plants.

Next to costs, we also touch upon the associated CO_2 emissions for each of the routes (Chapter 4). This greenhouse gas performance is important to understand the feasibility of the electrochemical routes in comparison to conventional fossil-based approaches. In Chapter 5, we provide an overview of knowledge gaps and research questions before presenting the conclusions in Chapter 6. We hope that the insight from our assessment helps people from universities, knowledge institutes, industry, and governments to steer developments in the right direction and to accelerate industrial transformation.

2 State-of-the-art

Electrochemistry may appear as an attractive approach to convert a stable molecule like CO_2 into an array of carbon-based products, such as CO, FA, and C_2H_4. Here we investigate six routes to electrochemically convert CO_2 to produce CO (2 routes), syngas (1 route), formic acid (1 route), and ethylene (2 routes). In these routes, two key technologies are applied, *i.e.* low temperature (LT) electrolysis and high temperature (HT) electrolysis. We first determine the technical status of the involved technology in terms of system size and configuration, energy and mass balances, current investment costs, technology readiness level (TRL) and existing projects. Electrochemical CO_2 conversion processes are currently not industrially applied and we include the commercial chlor-alkali process as a reference and benchmark technology in our analysis. The methodology for our analysis has been described in more detail in the ESI.†

2.1 Chlor-alkali process

The chlor-alkali electrolytic process is globally the main technology to produce chlorine and caustic soda. Three types of systems are widely applied: the mercury cell, diaphragm cell and membrane cell. The first two were commercialized in the late 19th century, while the membrane cell process was developed in the 1950s.[17,18] Due to concerns around the use of mercury and asbestos in mercury and diaphragm cells respectively, the membrane cell process has become the dominant technology, possessing in the EU-27 a 60% share for chlorine production in 2012,[19] and an 85% share in 2019.[20] In all three processes, an electric potential is applied onto two electrodes to convert sodium chloride and water into sodium hydroxide, chlorine, and hydrogen (eqn (1)).

$$2NaCl + 2H_2O \rightarrow 2NaOH + Cl_2 + H_2 \quad (1)$$

Another novel approach has recently entered the market, the so-called oxygen-depolarised cathode (ODC) cell, which is an update of the membrane cell approach. Rather than co-producing H_2, ODC cells consume O_2 at the cathode (eqn (2)). This process benefits from a lower cell voltage (from around 3.0 V down to 2.0 V in the ODC) process and thereby reduces the total energy requirements by around 25% (per kg Cl_2 produced).[21] A schematic design and operation of an electrolysis cell is given in the ESI (Fig. S2†).

$$2NaCl + H_2O + 1/2O_2 \rightarrow Cl_2 + 2NaOH \quad (2)$$

Globally, around 90 Mt Cl_2 is annually produced next to around 100 Mt of caustic soda.[22] To produce such an amount with an average stack electricity use of 2.4 MW h per ton of Cl_2, a total worldwide installed electrolyser capacity of around 27 GW is required (at a 90% load factor). This capacity (mainly membrane technology) will likely increase to fulfil the chlorine demand of a growing chemical industry.[20] Chlor-alkali electrolysis produces as a by-product around 2% of total global hydrogen.[23] The equipment is supplied by several manufacturers around the world, such as Thyssenkrupp.[24] These companies will likely also provide equipment for the water electrolyser industry and currently their combined annual equipment production capacity is roughly 2–3 GW per year in 2020.[25–27] This capacity has substantially increased over the last years because many companies are preparing themselves for a rapidly increasing demand for electrolysers.

The mass and energy balances of the current membrane electrolysis chlor-alkali process are summarised in the diagram in Fig. 2.

The complete chlor-alkali process starts from the NaCl salt and purified water. These two elements undergo a preparation process to produce the brine stream (concentrated aqueous salt solution) that will feed the electrolysis unit. The brine stream, along with the electricity input, yields the electrolysis process possible, producing a gaseous Cl_2 stream (anode side), H_2 (cathode side), and a concentrated aqueous caustic soda (NaOH) stream at the cathode. A post-treatment step for all three streams renders the final Cl_2 product, a 50% NaOH (aq.)

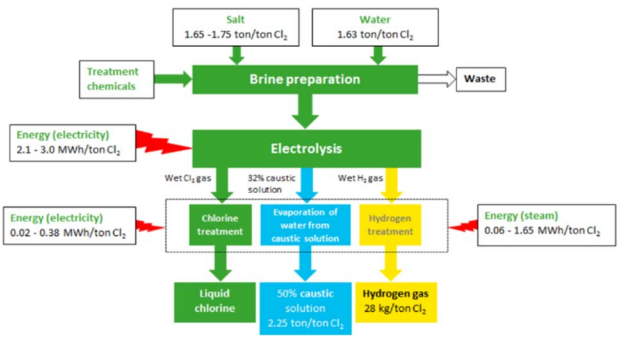

Fig. 2 Overview of the chlor-alkali production process and the main material flows (reproduced from ref. 22).

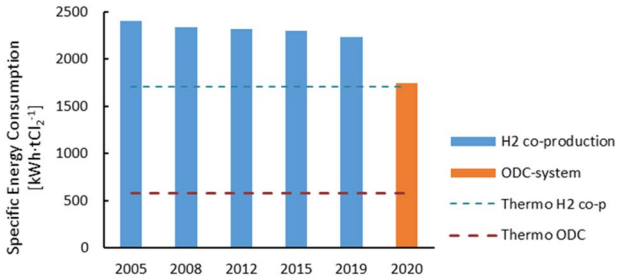

Fig. 3 Evolution of the specific energy consumption for the production of Cl_2 through the membrane electrolysis technology since 2005. H_2 co-production is the conventional technology seen in Fig. 2 and the oxygen depolarised cathode (ODC) technology represents a novel design in which oxygen is used at the cathode. Plot constructed with data from ref. 14 and 17.

solution, and some H_2 gas. A more detailed mass and energy balance is provided in the ESI (Table S2†).

The membrane electrolysis technology for the chlor-alkali process has undergone an optimisation process in terms of energy consumption, with new cell designs over the past 15 years. The new ODC design also represents a major improvement in the energy consumption for the chlor-alkali process (Fig. 3). The thermodynamic minimal energy requirements for both the H_2 co-production system and the ODC design are indicated by the striped lines, showing the maximal optimisation potential of both technologies.

2.2 Route 1: low-temperature CO_2 electroconversion to carbon monoxide

The LT electrochemical reduction of CO_2 into carbon monoxide (CO) consists of the electrolysis unit and a series of auxiliary units for the final production of a purified gaseous CO stream. A simplified process diagram is shown in Fig. 4. The overall reaction of the process is displayed in eqn (3). As is shown, CO_2 is the only reactant in the process, yielding CO and O_2.

$$CO_2 \rightarrow CO + 1/2O_2 \quad (3)$$

The current state of development for the LT CO_2 conversion to CO technology is estimated to be at a TRL 5–6.[28] In the Rheticus project, a joint venture between Siemens and Evonik, this process route is followed by a downstream unit that produces alcohols from the upstream electrochemical CO.[29] The aim of this project is the construction and validation of a 25 kW

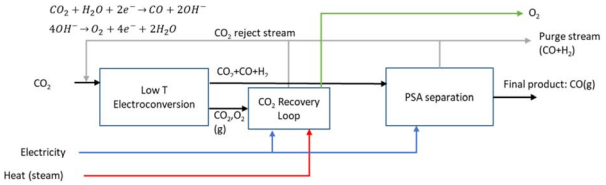

Fig. 4 Process diagram of the LT CO_2 electrolysis towards CO.

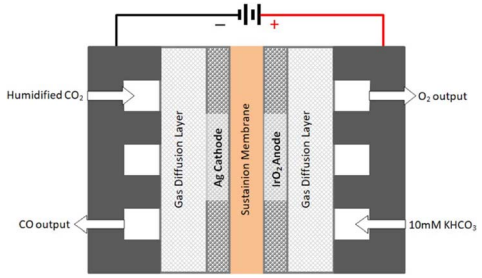

Fig. 5 Schematics of a typical membrane electrode assembly (MEA) cell for CO_2 electrolysis to CO (reproduced from Liu *et al.*, 2018).[34]

electrolyser stack for the production of syngas (CO + H_2), which will be fed to a bio-reactor for the fermentation into butanol and hexanol.

The technology involves the use of gas diffusion electrodes (GDEs) in a membrane electrode assembly (MEA) cell architecture, inspired by the PEM water electrolyser design.[30] An anion exchange membrane (AEM) is used to allow ionic transport. A gaseous, humidified CO_2 stream is fed at the back of the cathode GDE, producing CO and (undesired) H_2 through the hydrogen evolution reaction. The cathode outlet stream contains CO_2, H_2O, CO and H_2. A depiction of the MEA cell for LT CO_2 to CO is shown in Fig. 5.

The alkaline nature of the cathode acts as a trap for the fed CO_2, converting it into carbonates. The negatively charged carbonates cross the AEM and end up in the anode compartment. There, given the acidic nature of the anode environment, carbonates are acidified and CO_2 is released, along with O_2, produced through water oxidation. A neutral anolyte can be used to supply water to the anode.

The CO_2 utilisation degree (CO_2UD) determines the extent to which CO_2 is effectively converted to the product of interest. It is defined as the molar ratio of the CO_2 converted to the product of interest and the total CO_2 inlet to the cathode. The CO_2UD can be calculated as the ratio of the faradaic efficiency (FE), defined as the efficiency with which electrons participate in a given electrochemical transformation, towards the product and the total CO_2 consumed, as reported by Yang *et al.*[31] In neutral or alkaline media, a theoretical maximum of CO_2UD of 50% can be hypothesised for a 100% FE towards CO because of the concomitant formation of OH^-. The latter reacts with CO_2 to form HCO_3^- and CO_3^{2-} ions.

$$CO_2UD\left[\frac{\text{mol product}}{\text{mol } CO_2 \text{ in}}\right] = \frac{FE_{product}}{CO_2 \text{ consumed}} \leq 50\% \text{ for } CO_2 \rightarrow CO \quad (4)$$

The gas outlet from the anode side will contain O_2, CO_2 and some H_2O. Given the high O_2 concentration in this stream, CO_2 needs to be captured in an oxidation-resistant process, like a calcium caustic loop, used for direct air capture (DAC). Data were retrieved from Keith *et al.*[32] for a caustic loop consisting of three steps: a pellet reactor, calciner, and slaker. We assume that the modelled loop for CO_2 reclaiming uses electric energy

Table 2 State-of-the-art process parameters for LT electrolysis of CO_2 to CO

Parameter	Unit	Value	Ref.
Current density	A m^{-2}	2000	34
Cell voltage	V	3.0	34
Faradaic efficiency CO	—	98%	34
CO_2 utilisation degree	$mol_{CO}/mol_{CO_2\ in}$	49%	31
Carbon yield	$mol_{CO}/mol_{CO_2\ reduced}$	100%	Assumed
Power density	kW m^{-2}	6.0	Calculated
Stack lifetime	h	40 000	35

as input for the HT steps and has as outputs a gas stream of CO_2, which is recycled back to the cathode inlet of the LT electrolyser, and an O_2 gas stream.

On the cathode outlet, a mixture of CO_2 and CO (and traces of H_2 and H_2O) is sent to a pressure swing adsorption (PSA) unit for CO purification. The PSA unit delivers a commercial grade 98 vol% CO stream[33] as the final output and a reject stream with CO_2 and CO, which can be recycled to the electrolyser unit. In our calculations, the energy for this process is provided by electricity.

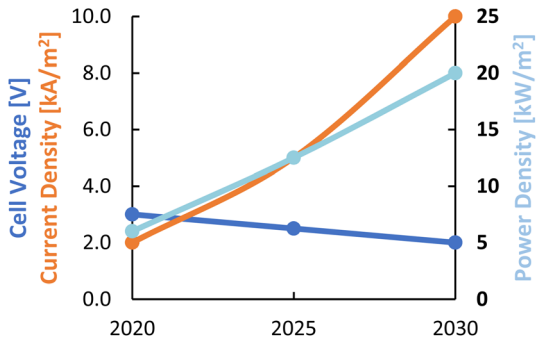

Fig. 6 Roadmap for different process performance indicators for LT CO_2 electrolysis for the current decade. Considered products are CO, FA, and C_2H_4. Reproduced from ref. 28.

Typical process performance indicators for the LT electrolysis of CO_2 to CO are reported in Table 2. At a cell voltage of around 3.0 V, the current density amounts to roughly 2000 A m^{-2}, which is an order of magnitude lower than that observed for PEM water electrolysis. The CO_2 utilisation degree depends on the FE and is close to its limit of 50% (see eqn (4)). We assume that the net carbon yield is 100%, which means that all CO_2 ends up either in the product or else is recycled in the process. In reality, a fraction of the carbon is likely lost in the purge stream. The production of 1 kg of CO requires around 1.6 kg of CO_2 and uses approximately 7.2 kW h of electricity. More detailed mass and energy balances of the process are shown in Table S3, while information concerning material use is provided in Table S10 (see the ESI).†

Expectations are that these performance parameters for LT CO_2 electrolysis towards different products can be improved significantly. The development targets, in terms of current density, cell voltage, and power density for the current decade are described by Nørskov *et al.*[28] and plotted in Fig. 6. The expected performance of LT CO_2 electrolysis by 2030 will approach that of the current PEM water electrolysis technology in terms of current density and power density. The power density variable is the product of the cell voltage and the partial current density (FE times total current density) towards the product of interest and is a measure of the productivity of the cell in terms of delivered power per unit of electrode area.

Our estimate of the investment costs for LT CO_2 electrolysers is based on PEM water electrolysis, as the most comparable commercial technology available. The electrolysis unit investment costs are reported as a function of the total electrical installed capacity. The stack lifetime for the LT CO_2 electrolysis stacks is taken from the PEM water electrolysis technology, given the lack of data on long-term testing of this process under industrially relevant conditions. An overview of long-term performance data for several electrolysis technologies is given by Küngas,[30] reporting >4000 h of operation for an LT CO_2 electrolysis unit for CO production. A summary of the different cost indicators is presented in Table 3. Given the different power densities for PEM water electrolysis and LT CO_2 electrolysis, the reported values for investment costs for the PEM

Table 3 Investment costs for LT CO_2 electrolysis to produce CO

Parameter	Unit	Value	Ref.
Total PEM electrolysis system (uninstalled costs)[a]	€ per kW	667–1450	38
Stack cost share[b]	—	60%	39
Power electronics cost share[b]	—	15%	39
Gas conditioning cost share[b]	—	10%	39
Balance of plant cost share[b]	—	15%	39
Power density PEM electrolysis[c]	kW m^{-2}	29	40
Total LT CO_2 electrolysis system (uninstalled costs)	€ per kW	3200–7000	This study
Calcium caustic recovery loop unit	€ per kW	2100	32
PSA CO/CO_2 separation unit	€ per kW	540	36 and 37
LT CO_2 electrolysis plant to produce CO (total investment costs)	€ per kW	11 700–19 000	This study

[a] Approximate uninstalled investment costs for a PEM electrolysis unit (stack and auxiliary equipment) for a 1 MW electrolysis unit in 2019. [b] The cost share of the different components reported by Böhm *et al.*[39] refer to the first row of the table. [c] The '*power density*' factor for PEM electrolysis is reported by Mayyas *et al.*[40] for a PEM system with a performance of 17 kA m^{-2} at 1.7 V total cell voltage.

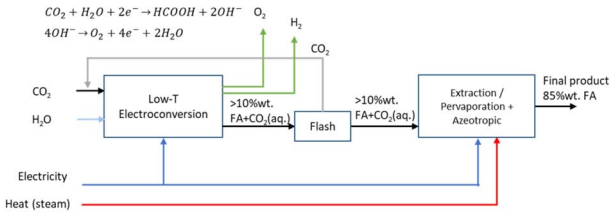

Fig. 7 Process diagram of the LT CO_2 electrolysis towards FA.

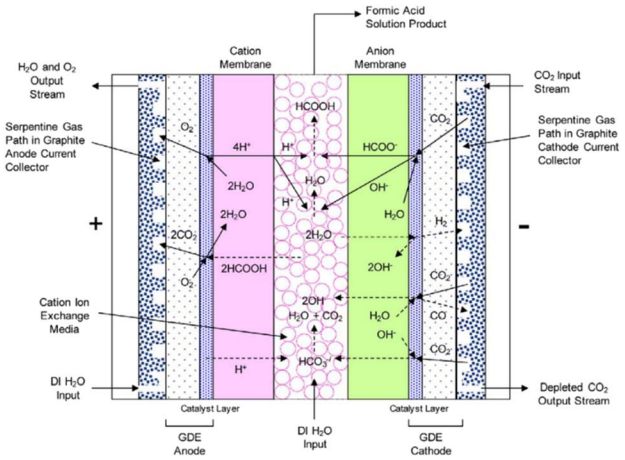

Fig. 8 Schematic representation of the 3-compartment electrochemical cell for the direct production of FA through an LT CO_2 electrolysis process, showing proposed electrochemical reactions and ion transport. Reproduced from Yang *et al.*, 2017.[46]

systems have been adapted to the performance indicators for LT CO_2 electrolysis (see also ESI, eqn (5)).† The specific capital expenditure (CAPEX) for the LT CO_2 electrolysis system amounts to 3200–7000€ per kW. The investment costs for the calcium caustic recovery loop for CO_2 recovery from the anode side are based on a 235 M€ investment for a 123 t_{CO_2} per h capture system.[32] The PSA unit for CO purification costs around 1.7 M€ for 1000 Nm^3 h^{-1}.[36,37] CAPEX for these two units is adapted to the size of our LT CO production plant using a scaling factor of 0.7.[36] The total investment costs for the LT CO_2 electrolysis to CO facility are calculated by applying an installation factor of 1.8 and adding 10% owner's costs over the installed costs and amount to 11 700–19 000€ per kW.

2.3 Route 2: low-temperature CO_2 electroconversion to formic acid

The LT electrochemical reduction of CO_2 into formic acid/formate consists of an electrolysis unit and a series of auxiliary units for the final production of a purified aqueous FA stream. A diagram of the complete process is shown in Fig. 7. The overall reaction process is displayed in eqn (5). The reactants CO_2 and H_2O are converted in the process into FA and O_2.

$$CO_2 + H_2O \rightarrow FA + 1/2O_2 \quad (5)$$

The current development stage for the LT CO_2 conversion to FA is claimed to be at a TRL 3–5.[41] The most important projects that aim to bring this process route to the next level are summarised in Table 4. The state-of-the-art for LT electrolysis of CO_2 to FA involves the use of GDEs and a special electrochemical cell design with an acidic centre compartment for the direct production of FA and not the deprotonated formate ($HCOO^-$). The production of $HCOO^-$ requires a costly downstream protonation step with, for instance, an electrodialysis process to generate FA, as reported by Ramdin *et al.*[42]

An electrochemical cell design that is reported to directly produce a diluted (up to 10 wt%) FA aqueous stream is reported by Yang *et al.*[47] The cell is a 3-compartment electrolyser, featuring a cathode GDE for the conversion of gaseous CO_2 to $HCOO^-$ and an AEM directly attached to the cathode GDE that allows for the direct migration of $HCOO^-$ anions towards the centre compartment. In the middle compartment, acid cation exchange media are present to provide both electrical conductivity and protons to form FA from $HCOO^-$. On the other side, an anode GDE compartment is fed with liquid water for O_2 production. This GDE is directly attached to a CEM to allow for

Table 4 Summary of the most important development projects for LT CO_2 to FA

Project	Framework	Involvement	Description
OCEAN[a]	ASPIRE	AVANTIUM, ERIC, IIT, Gaskatel, Politecnico di Torino, RWE, Universiteit van Amsterdam	Achieve a TRL 6 development stage for the electrochemical conversion of CO_2 to formate (250 g h^{-1} at 1500 A m^{-2})
e2C[b]	Interreg 2-Seas	TNO, VITO, Universiteit Antwerp, Lille University, University of Sheffield, University of Exeter, TU Delft	Build a pilot demonstrator for the LT CO_2 conversion to FA and validate the technology at TRL 6
ECFORM[c]	—	DNV GL	Semi-pilot ECFORM demonstration reactor with a 600 cm^2 surface area and a capacity of reducing approximately 1 kg CO_2 per day and producing formic acid (85 wt%)

[a] OCEAN (2022).[43] [b] e2C (2022).[44] [c] Zhu (2019).[45]

Table 5 State-of-the-art process parameters for LT electrolysis of CO_2 to FA

Parameter	Unit	Value	Ref.
Current density	A m^{-2}	2000	47
Cell voltage	V	3.75	47
Faradaic efficiency FA	—	73–91%	47
CO_2 utilisation degree	$mol_{FA}/mol_{CO_2\ in}$	37–46%	47
Carbon yield	$mol_{FA}/mol_{CO_2\ reduced}$	100%	Assumed
Power density	kW m^{-2}	7.5	Calculated
Stack lifetime	h	40 000	35

the transport of protons from the oxygen evolution reaction at the anode towards the centre compartment. The sketch of the said cell design is shown in Fig. 8.

Analogously as for the LT CO_2 to CO route, some CO_2 will migrate from the gas compartment to the electrolyser in the form of (bi)carbonates. The CO_2UD can also be assumed as half of the FE towards FA. The (bi)carbonate anions will cross towards the middle compartment, and, given the acidic nature of the latter (pH of *ca.* 1.0 for 10 wt% FA concentration),[47] CO_2 will be stripped out from this compartment, which can be easily separated from the aqueous FA stream with a flash unit, as seen in Fig. 7. Therefore, there is no need of adding a CO_2 recovery loop for the anode outlet stream, as for the LT CO_2 to CO route. The outlet FA stream from the flash unit is fed to a hybrid extraction–distillation process to achieve industrially relevant concentrations of FA > 85 wt% (aq.), as proposed by Ramdin *et al.*[42] A simplified process flow diagram of this purification section is depicted in the ESI (Fig. S3†).

Our selected state-of-the-art process performance indicators for the LT electrolysis of CO_2 to FA are reported in Table 5. The typical current density of 2000 A m^{-2} is in the same order of magnitude as for the CO process, but the required cell voltage of 3.75 V is slightly higher. The FE is slightly lower compared to that for CO production, because in the FA process also some H_2 is formed. The CO_2 utilisation degree is dependent on the FE towards FA, and consequently lower as for the CO case. The production of 1 kg of aq. 85 wt% FA solution requires around 0.81 kg of CO_2 and uses approximately 6.0 kW h of electricity. More detailed mass and energy balances of the process and material use are shown in Tables S4 and S10,† respectively.

CAPEX for the electrolysis unit for the LT CO_2 electrolysis to FA is determined analogously as for the LT CO_2 to CO case (see Table 3), by using the power density of the FA production process. The specific CAPEX for the LT CO_2 electrolysis system amounts to 2700–5700€ per kW (Table 6). The costs for the additional cation exchange membrane (107€ per kW) have been included.[112] The costs of a downstream hybrid extraction and

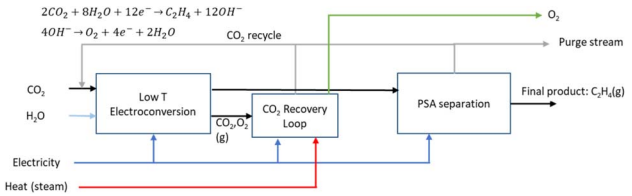

Fig. 9 Process diagram of the LT CO_2 electrolysis towards C_2H_4.

distillation train for formic acid purification have been described for a 1.0 t_{CO_2} per h system and come to 7.9 M€.[42] This system is scaled to the required size (scaling factor 0.7) and added to the total equipment costs. After correction for total project costs (installation factor 2.0), the total investment costs for the LT CO_2 electrolysis to FA facility amount to 10 700–16 700€ per kW.

2.4 Route 3: low-temperature CO_2 electroconversion to ethylene

The LT electrochemical reduction of CO_2 into ethylene (C_2H_4) consists of an electrolysis unit, and a series of auxiliary units for the final production of a purified gaseous C_2H_4 stream. A diagram of the complete process is shown in Fig. 9. In the chemical reaction CO_2 and H_2O are converted into C_2H_4 and O_2, as depicted in eqn (6).

$$2CO_2 + 2H_2O \rightarrow C_2H_4 + 3O_2 \quad (6)$$

LT CO_2 conversion to C_2H_4 technology is being validated in the laboratory, which implies a TRL of 3–4.[41] In two European projects this process route is further developed (Table 7). Currently, GDEs and a MEA-type of cell design are typically used, analogous to that for LT CO production (see Fig. 5). In the LT C_2H_4 case, a humidified CO_2 gas stream is fed to the cathode GDE, which is separated with an AEM from the anode side. At the anode, an alkaline aqueous stream is fed to sustain the oxygen evolution reaction. The cathode outlet stream contains CO_2, H_2O, C_2H_4, other C-gaseous products, possible C-liquid products, and H_2. A depiction of the MEA cell for LT CO_2 to C_2H_4 is shown in Fig. 10.

During the formation of a single molecule of C_2H_4, 12 electrons and 12 OH^- molecules are produced. These hydroxides generate a highly alkaline environment at the cathode and act as a trap for the fed CO_2, converting it into carbonates. As for the LT CO production case, these carbonates can migrate through the AEM towards the anode side. The CO_2 lost to CO_2 reacted ratio is even higher than for the LT CO scenario. Gabardo *et al.*

Table 6 Investment costs for LT CO_2 electrolysis to produce FA

Parameter	Unit	Value	Ref.
Total LT CO_2 electrolysis system (uninstalled costs)	€ per kW	2700–5700	This study
Hybrid extraction + distillation train	€ per kW	2700	42
LT CO_2 electrolysis plant to produce FA (total investment costs)	€ perkW	10 700–16 700	This study

Table 7 Summary of the most important development projects for LT CO_2 to C_2H_4

Project	Framework	Involvement	Description
SELECT CO_2[a]	EU Horizon 2020	TU Berlin, EPFL, TU Delft, RINA, DTU, De Nora, Pretexo, University of Surrey, SLAC	Development of LT CO_2 electrolysis technology to achieve TRL 4 for C_2H_4 production
Electrochemical CO_2 reduction to ethylene for industrial applications[b]	Energi forskning	Siemens, DTU	Joint Siemens & DTU project for large-scale production of a generic electrode platform for electrochemical reduction of CO_2 to ethylene

[a] SELECT CO_2 (2022).[48] [b] Energiforskning (2022).[49]

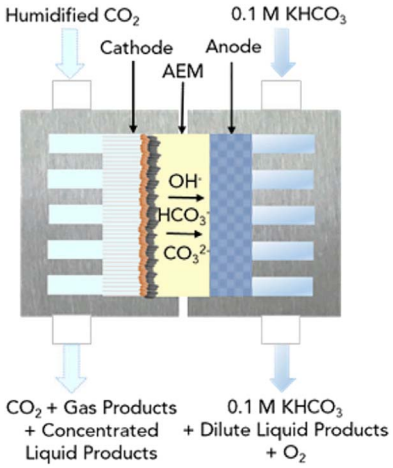

Fig. 10 Schematic diagram of the MEA cell for the LT electrolysis of CO_2 to C_2H_4. Reproduced from Gabardo *et al.* (2019).[50]

reported a 4 : 1 ratio for the CO_2 lost to CO_2 reacted (*i.e.*, $CO_2UD = 20\%$).[50] Sisler *et al.* report a more optimistic scenario of a 2 : 1 ratio ($CO_2UD = 33\%$).[51] Due to the CO_2 crossover from the cathode to the anode, the gas outlet from the anode side contains O_2, CO_2 and some H_2O. A calcium caustic recovery loop for CO_2 reclaiming is considered, as it was done for the LT CO case. The recovered CO_2 from this loop will be fed back to the cathode inlet of the LT electrolyser. On the cathode outlet, a mixture of CO_2, C_2H_4, and traces of H_2 and H_2O is sent to a PSA unit for C_2H_4 purification. The final outputs from this PSA unit will be a commercial grade 99.9 wt% C_2H_4 stream,[52] and a reject stream with CO_2 and C_2H_4. A simplified process diagram of the complete LT C_2H_4 production process is shown in Fig. 11.

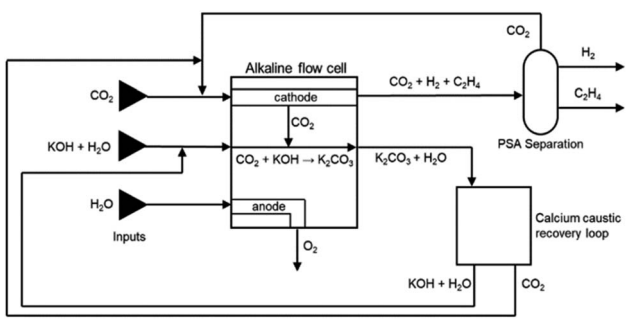

Fig. 11 Process flow diagram for CO_2 reduction towards ethylene in an alkaline flow cell. Reproduced from Sisler *et al.* (2021).[51]

Current state-of-the-art process performance indicators for the LT electrolysis of CO_2 to C_2H_4 are reported in Table 8. The current density of 1200 A m^{-2} is slightly lower in comparison to the processes to produce CO and FA. The cell voltage of 3.7 V is similar to that of electrochemical FA production. The co-production of hydrogen and other carbon-based compounds lowers the FE towards the desired product, C_2H_4. Also, the carbon yield is below 100% because some side-products are formed, such as CO and ethanol. The production of 1 kg of C_2H_4 consumes approximately 4.7 kg of CO_2 and 80 kW h of electricity. The overall C_2H_4 yield could potentially be enhanced by feeding the electrochemical cell with a CO_2–CO mixture, as there is no site competition between both reactants on the reactive catalyst surface. Therefore, C_2H_4 could be produced electrochemically from an impure CO_2 stream containing CO, which is quite common at an industrial scale for CO_2 feeds.[53] The complete mass and energy balances for the LT electrolysis of CO_2 to C_2H_4 process are shown in Table S5 and information on the use of materials is provided in Table S10 (see the ESI).†

The estimation of the investment costs for the electrolysis unit for the LT CO_2 electrolysis to ethylene is done analogously to the previous routes (see Tables 3 and 6). The PSA unit is based on data from the LT CO_2 to CO case (Table 3) and adapted to the present route. Total specific investment costs for the plant amount to 10 300–20 400€ per kW (Table 9).

2.5 Route 4: high-temperature solid oxide CO_2 electroconversion to carbon monoxide

High-temperature (HT) electrolysis in a solid oxide electrolyser (SOE) is the only CO_2 electrolysis technology that is approaching commercialization (TRL 8).[30] The technology is based on solid oxide cell (SOC) technology presented in Fig. 12, composed of ceramic-based components (cathode and anode electrodes and electrolyte) able to produce CO *via* the electrolysis of CO_2 at elevated temperatures (600–800 °C). According to the SOC principle, CO_2 is fed to the cathode side of the cell *via* gas channels, which helps to distribute the gas across the cell. In the porous cathode (fuel electrode) CO_2 is reduced to CO. The electrons for the reaction are provided by an external power

Table 8 State-of-the-art process parameters for LT electrolysis of CO_2 to C_2H_4

Parameter	Unit	Value	Ref.
Current density	A m^{-2}	1200	54
Cell voltage	V	3.70	53
Faradaic efficiency	—	64% (C_2H_4) 74% (all C_{prod})	53
CO_2 utilisation degree	$mol_{C_2H_4}/mol_{CO_2\ in}$	20%	53
Carbon yield[a]	$mol_{C_2H_4}/mol_{CO_2\ reduced}$	86%	Calculated
Power density	kW m^{-2}	4.4	Calculated
Stack lifetime	h	40 000	35

[a] The carbon yield to product is calculated as the ratio between the FE towards C_2H_4, and the FE towards all carbon-products (C_{prod}, incl. C_2H_4).

Table 9 Investment costs for LT CO_2 electrolysis to produce C_2H_4

Parameter	Unit	Value	Ref.
Total LT CO_2 electrolysis system (uninstalled costs)	€ per kW	4400–9600	This study
Calcium caustic recovery loop unit	€ per kW	580	32
PSA CO/CO_2 separation unit	€ per kW	200	36 and 37
LT CO_2 electrolysis plant to produce C_2H_4 (total investment costs)	€ per kW	10 300–20 400	This study

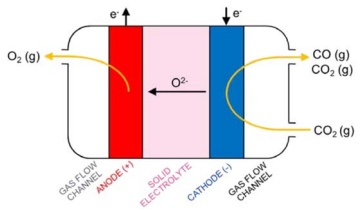

Fig. 12 Principle of CO production in a solid oxide cell (Küngas, 2020).[30]

supply. The oxide ions (O^{2-}) formed in the reaction are incorporated into the electrolyte and traverse through the electrode into the anode, where the ions are oxidized into molecular oxygen.[30]

The SOE concept for CO production has been exclusively developed on the system scale by the technology supplier Topsøe.[30] Topsøe technology is based on electrode-supported SOC technology (Fig. 13, top left), operating at a temperature of 700 °C, thanks to the thin Yttria-stabilized zirconia (YSZ) electrolyte design allowing the conduction of O^{2-} ions at this temperature with a low internal resistance, a Ni-YSZ fuel electrode cermet (cathode) able to convert CO_2 into CO and a perovskite-based anode La0.6Sr0.4Co0.2Fe0.8O3- (Ce0.9Gd0.1)O1.95 (LSCF-CGO) able to reconvert O^{2-} ions into O_2 (see also Table S10†). All layers constitute the core of the single repeating SOC units assembled in a stack design (Fig. 13) with the addition of metallic-based bipolar separators and end plates enabling gas and current transfer through the cell and stack and sealing components next to each bipolar separator plate to prevent gas-crossing between the anode and cathode sides.

Topsøe developed this stack technology for direct implementation on the system level for CO production at an industrial site, in a stand-alone unit connected with power, CO_2, and product gas, as shown in Fig. 14. It can produce on-demand capacities ranging from 1 to 250 kg h^{-1} of CO.

Single-pass conversion of CO_2 to CO depends on the operating temperature of the SOE stack (Duhn, 2017).[56] The limitation for high single-pass conversion of CO_2 is due to carbon formation by the Boudouard reaction and resulting degradation of the cell. For the base case, a single-pass CO_2 conversion of 50% is assumed and the overall conversion is assumed to be 100%. Hence, on a system level, 1 mole of CO_2 will produce 1

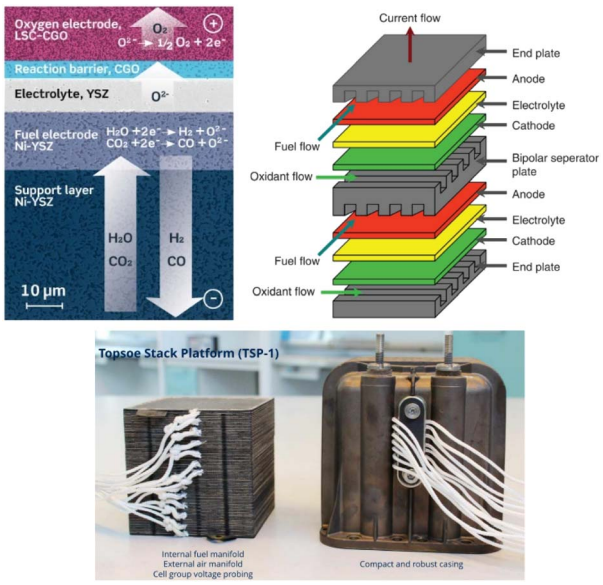

Fig. 13 Top left: electrode supported solid oxide cell design (reproduced from Hauch *et al.*, 2020),[55] top right: scheme of two single repeating SOC units design in a SOE stack (reproduced from Singhal, 2014),[56] bottom left: Topsøe stack design developed for CO production (reproduced from Küngas *et al.*, 2019).[58]

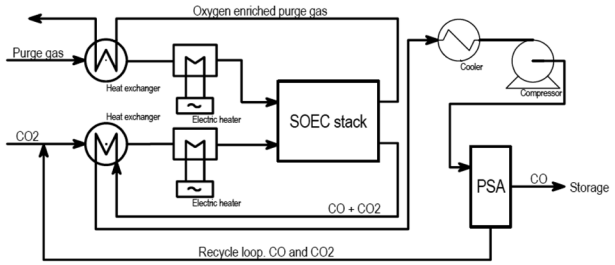

Fig. 14 Block flow diagram for Topsøe's eCOS unit for the SOE CO_2 to CO process (Duhn, 2017).[57]

Table 10 State-of-the-art process parameters for HT electrolysis of CO_2 to CO

Parameter	Unit	Value	Ref.
Current density	A m^{-2}	7500	60
Cell voltage	V	1.5	59
Faradaic efficiency CO	—	100%	30
CO_2 utilisation degree	$mol_{CO}/mol_{CO_2\ in}$	<60%	56
Carbon yield	$mol_{CO}/mol_{CO_2\ reduced}$	100%	Assumed
Power density	kW m^{-2}	11	Calculated
Stack lifetime	h	8000	57

mole of CO. The electric power consumption for the stack varies between 2.6 and 2.8 kW h kg^{-1} of CO and depends on the operating voltage.[58] Total system energy consumption depends on the level of heat integration and single-pass CO_2 conversion. The total energy consumption for the system will be between 4.7 and 6.3 kW h per kg CO produced. Based on stoichiometry, for 1 mole of CO produced, 0.5 mole of oxygen will be produced. The oxygen has to be diluted in the process with sweep air due to safety issues in the stack. In the PSA unit, there will be a trade-off between yield and purity of CO.[59] We assume a commercial grade CO product purity of around 98 vol%, analogously to the LT CO production process.[33] Current process performance parameters for CO production are shown in Table 10. The current density of 7500 A m^{-2} is almost four times higher in comparison to the LT process (Table 3), while the cell voltage remains at around 1.4 V. This results in a power density of 11 kW m^{-2} for the HT process. The stack lifetime is estimated to be around 8000 hours.[57] The overall mass and energy balance for the CO_2-SOE production system is shown in Table S6.†

The total uninstalled CAPEX for the system is calculated based on the steam electrolysis data taken from Hydrogen Europe targets. Here, the system capacity is assumed to be 1 MW_e. The split of CAPEX was assumed to be 30% for the cell stack, 30% for the power electronics, 6% for the gas conditioning, and 34% for the balance of plant.[39] CAPEX for CO_2 electrolysis is scaled based on the ratio of power density (kW m^{-2}) for steam and CO_2 electrolysis. Further, CO_2 electrolysis will require an additional PSA separation unit compared to steam electrolysis. CAPEX of 600€ per kW for the PSA unit has been calculated by taking the total flow rate of CO_2 and CO entering the PSA unit as basis.[37] The total investment costs of CO_2-SOE systems for CO production amount to 4200–6600€ per kW. A summary of the different cost indicators is presented in Table 11.

Despite achieving high TRL completion (TRL8) for CO production, SOE technology shows constant development at the cell, stack and system levels to reduce system costs for viable commercial implementation in the industrial sector (TRL9). CAPEX cost reduction can be achieved through the reduction of critical raw material (CRM) content (*e.g.* Co, Sr, Y…) in the SOE cell manufacturing,[62,63] reduction of stack (<150k€ per kW) and system (<500k€ per kW) costs[64] and improvement of the yield of production for mass integration in the industry,[65] while improving efficiency of the SOE cell (high current density operations), stack (high fuel utilization) and system (heat & gas recycling) components.

OPEX reduction is aimed at by increasing the SOE cells and stack lifetime (≫ 8000 h) with the prevention of the coking process (Boudouard reaction) and sulphur poisoning at the fuel electrode (cathode) side. This can be realized through optimization of the robustness of the cell and stack components & design, with the development of alternative materials compared to the highly reactive state-of-the-art Ni-YSZ cermet fuel electrode.[66] Tuning of the operating conditions of the SOE stack (temperature, pressure, current density) and integration of purification systems (desulfurization) in the BoP of the SOE system are also under development to prevent poisoning issues at the fuel side of the stack.[67]

Table 11 Investment costs for the HT CO_2-SOE plant to produce CO

Parameter	Unit	Value	Ref.
Total SOE system (uninstalled costs)[a]	€ per kW	520–2130	61
Stack cost share[b]	—	30%	39
Power electronics cost share[b]	—	30%	39
Gas conditioning cost share[b]	—	6%	39
Balance of plant cost share[b]	—	34%	39
Power density SOE[c]	kW m^{-2}	11	59
Total HT CO_2-SOE system (uninstalled costs)	€ per kW	1500–2700	This study
PSA CO/CO_2 separation unit	€ per kW	600	36 and 37
HT CO_2-SOE plant to produce CO (total investment costs)	€ per kW	4200–6600	This study

[a] Approximate uninstalled investment costs for a SOE unit (stack and auxiliary equipment) for a 1 MW electrolysis unit in 2020. [b] The cost share of the different components reported by Böhm *et al.*[39] refer to the first row of the table. [c] The '*power density*' factor for SO electrolysis is reported by Foit *et al.*[59] for a SOE system with a performance of 7.5 kA m^{-2} at 1.5 V total cell voltage.

2.6 Route 5: high-temperature solid oxide CO_2 electroconversion to syngas

Syngas (H_2/CO) of tuneable ratios can be produced in one single electroconversion process step at HT with a similar operating principle in solid oxide cells to that used for CO production (as shown in Fig. 15). The operating concept of the SOE for syngas production consists of a co-electrolysis (co-SOE) of water and CO_2, able to produce variable H_2 and CO compositions, for further process applications, as for instance, production of green fuels and chemicals such as methane and methanol. Steam and CO_2 are reduced in the SOEC according to eqn (7), with the H_2/CO ratio in the syngas modified by variations of the steam and CO_2 flows.

$$CO_2 + H_2O \rightarrow CO + H_2 + O_2 \quad (7)$$

The production of syngas (H_2/CO) using co-SOE is in the development phase with an achieved TRL of 5 to 6. The German system supplier Sunfire is the world leader and is known as the only system supplier for co-SOE systems (Fig. 16).[68] The Sunfire system is based on a high-temperature operation (850 °C), with electrolyte-supported cells and stack technology (Fig. 17). The actual system is developed on a 150 kW scale, with the so-called name Syn-link (Fig. 17).

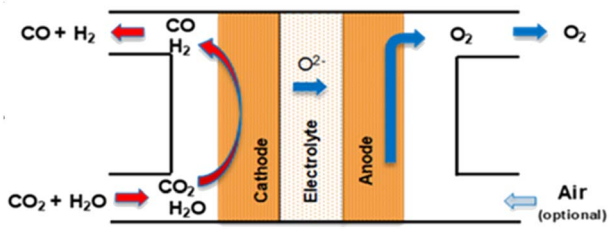

Fig. 15 Schematical concept of a SOE cell for HT co-electrolysis of steam and CO_2 to produce syngas.

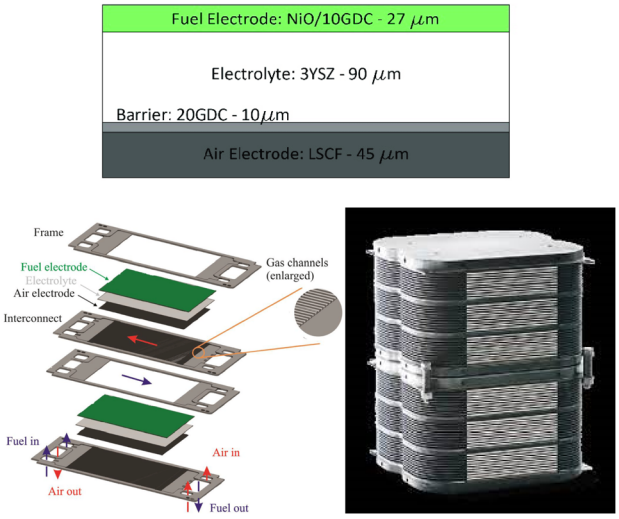

Fig. 16 Sunfire solid oxide cell and stack technology for co-SOE electrolysers (Masini *et al.*, 2019; Sunfire, 2022).[69,70]

Fig. 17 150 kW co-SOE Syn-link system developed at Sunfire (Sunfire, 2022).[71]

The co-SOE technology has been developed within multiple European research projects. To the best of our knowledge, the past and on-going projects for the development of co-SOE systems from kW to MW scale are summarized in Table 12.

For the calculations in this study, a syngas composition of $H_2 : CO = 2 : 1$ is assumed. This syngas ratio corresponds approximately to the ratio required for fuel production through the Fischer–Tropsch process and methanol synthesis. The mass balance for the base case is based on stoichiometry calculations. The operating conditions are similar to those of HT CO production, although the cell voltage is slightly lower, *i.e.* 1.3 V (Table 13). The single-pass conversion of CO_2 and H_2O for the base case is assumed to be 80%.[76] Fig. 18 shows the conceptual block flow diagram for syngas production using an HT SOE system.

The outlet gas mixture produced from SOE systems (H_2 : CO : CO_2 : steam) requires additional separation processes to feed clean syngas (H_2/CO) for the sub-mentioned fuels and chemical production processes (depending on the end-use of syngas). Steam is commonly removed by a condensation process and recycled into the steam system. CO_2 can be separated from the ($H_2 : CO : CO_2$) gas stream by absorption, adsorption, or membrane-based separation methods. Moreover, absorption-based separation with amine solutions is commercially available. Separated CO_2 is recycled to the inlet of the SOE system. However, the separation of CO_2 from syngas depends on the end-use of the produced syngas (for instance, for methanol production, the syngas inlet feedstock can contain CO_2). The heat from SOE outlet gases is recovered using heat exchangers to increase the overall system energy efficiency. The stack lifetime equals around 40 000 hours based on Posdziech,[77] which is substantially higher compared to the 8000 h reported by Topsøe for CO production.[57] This difference is explained by the degradation of the stack due to carbon formation in the latter process. The total electricity input for the plant to produce a kg of syngas is 8.1 kW h of which nearly 90% is consumed by the stack. The overall mass balance for syngas production is given in Table S7 and information about the materials used can be found in Table S10 (ESI).†

The total uninstalled CAPEX for the system is calculated based on steam electrolysis data taken from Hydrogen Europe[60]

Table 12 Summary of the most important development projects for HT electrochemical CO_2 conversion

Project	Period	Involvement	Description
Eco project[a]	2016–2019		co-SOE concept for methane production
Kopernikus[b]	2016–2019	Sunfire	Development of a 10 kW co-SOE system by Sunfire
Norsk e-fuel[c]	2019–2025		Development of the co-SOE technology for production of green-fuel for aviation & maritime transport, from CO_2 captured from the air and renewable energy sources
MegaSyn[d]	2021–2025	FCHJU project	Demonstration of large-scale co-electrolysis for the industrial power-to-X market: first demonstration of syngas production by co-electrolysis on the mega-watt scale in an industrial environment at the Schwechat Refinery in Austria, with Sunfire technology

[a] Eco (2019).[72] [b] Kopernikus (2019).[73] [c] Norsk e-fuel (2022).[74] [d] MegaSyn (2022).[75]

Table 13 State-of-the-art process parameters for HT electrolysis of CO_2 to syngas

Parameter	Unit	Value	Ref.
Current density	A m^{-2}	7500	75
Cell voltage	V	1.3	75
Faradaic efficiency syngas	—	100%	Assumed
CO_2 utilisation degree	$mol_{CO}/mol_{CO_2\ in}$	80%	75
Carbon yield	$mol_{CO}/mol_{CO_2\ reduced}$	100%	Assumed
Power density	kW m^{-2}	9.9	Calculated
Stack lifetime	h	40 000	76

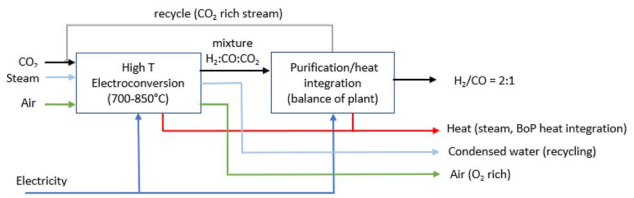

Fig. 18 Conceptual block flow diagram for the HT co-electrolysis process for syngas production.

targets in a similar fashion to that for CO production (see Table 11). Syngas electrolysis will likely require additional separation compared to steam electrolysis. CAPEX for the separation unit has not been included and, if deemed necessary, may increase the overall investment and production costs of this route. The total investment costs for a HT electrochemical syngas production plant range between 3000 and 5400€ per kW (Table 14).

Besides SOECs, molten carbonate electrolysis cells (MCECs) can also be applied to electrochemically produce CO or syngas at high temperatures (600–900 °C).[78] Although MCEC system development has only reached a TRL of 4, the use of this technology for syngas and CO production has a promising perspective for industrial implementation. This is because MCFC technology, the reversible MCEC concept, is already commercialized on an industrial scale (TRL 9) for power and heat generation with units of up to 3.7 MW sold by Fuel Cell Energy[79] and POSCO[80] and several power plants of 10–60 MW are already installed worldwide.[81] In our analysis, the MCEC concept is nevertheless not included as a separate route because, due to the development at low TRL, information on the system development (stack cost and effective operation) is

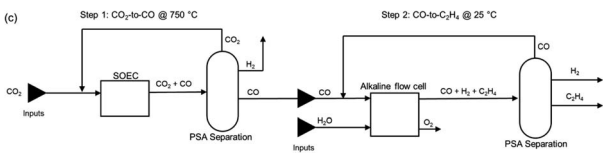

Fig. 19 Process diagram of the tandem HT CO_2 electrolysis to CO and LT CO electrolysis towards C_2H_4, the so-called tandem process. Adapted from Sisler *et al.*, 2021.[51]

Table 14 Investment costs for the HT CO_2-SOE plant to produce syngas

Parameter	Unit	Value	Ref.
Total HT CO_2-SOE system (uninstalled costs)	€ per kW	1500–2700	This study
HT CO_2-SOE plant to produce syngas (total investment costs)	€ per kW	3000–5400	This study

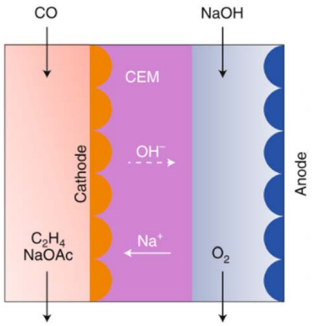

Fig. 20 CO electrolyser design for the production of C_2H_4, with a CEM and an alkaline anolyte for the OER. Reproduced from Jouny *et al.*, 2019.[82]

lacking. More details on the process and state-of-the-art can be found in the (ESI, Section 2.7).†

2.7 Route 6: tandem electroconversion approach to produce ethylene

The tandem process for the production of C_2H_4 consists of the combination of a HT electrolysis unit for CO_2 electrolysis towards CO (and the subsequent downstream processes for CO purification), followed by a LT electrolysis step for the conversion of the intermediate CO into C_2H_4, including auxiliary units for the purification and separation of C_2H_4. A diagram of the complete process is shown in Fig. 19. The individual reactions of the HT step and the LT step are displayed in eqn (8) and (9) below.

$$\text{Step 1: HT } CO_2 \text{ electrolysis: } 2CO_2 \rightarrow 2CO + O_2 \quad (8)$$

$$\text{Step 2: LT CO electrolysis: } 2CO + 2H_2O \rightarrow C_2H_4 + 2O_2 \quad (9)$$

The overall reaction of the tandem process, which is as expected equivalent to that of the LT CO_2 conversion route towards C_2H_4, is displayed in eqn (10).

$$2CO_2 + 2H_2O \rightarrow C_2H_4 + 3O_2 \quad (10)$$

The current development stage of the tandem route for C_2H_4 synthesis is limited by the LT conversion step, given that the HT step has already achieved a TRL 8–9 (see route 4). The LT CO electrolysis to products (C_{2+}, specifically C_2H_4) has been explored experimentally, and can be considered to be at a TRL 3.[82,83] The HT step for CO_2 electrolysis towards CO has already been discussed in route 4. LT electrolysis of CO to C_2H_4 comprises the use of a MEA cell design, in which a gaseous CO stream is fed to the electrolyser, to the gas side of the cathode GDE. The cathode is separated from the anode with an ion exchange membrane (either CEM or AEM). In the anode compartment, an alkaline anolyte is fed as a reactant for the OER. The cathode outlet stream contains CO, H_2O, C_2H_4, other C-gaseous products, possible C-liquid products, and H_2. A depiction of the MEA cell for LT CO to C_2H_4 is shown in Fig. 20.

In the HT step for CO_2 electrolysis towards CO, a PSA unit is included in the process diagram to allow for CO purification (see route 4). Also in the LT step for CO electrolysis, a PSA unit is included to ensure the required purity for the C_2H_4 gas stream (99.9 wt%, according to the NIH, 2022).[52]

Contrary to the LT CO_2 electrolysis routes, the nature of the LT CO electrolysis process does not allow for the formation of bicarbonates or any crossover of the cathodic reactant towards the anode, as stated by Sisler *et al.*[51] The fed CO in the second step of LT CO electrolysis will react electrochemically to form different CO reduction products, or it will leave the electrolyser unreacted, but it will not end up in the anode side. Therefore, there will be no need to implement a (CO) recovery loop in contrast to the CO_2 recovery step that is required for the LT CO_2 electrolysis towards C_2H_4 (see route 3). The process performance for the first electrolysis step is described in route 4. The second step, the LT electrolysis of CO to C_2H_4, is reported in Table 15. The total process to produce 1 kg of ethylene consumes 60–66 kW h of electricity of which approximately 85%

Table 15 State-of-the-art process parameters for LT electrolysis of CO to C_2H_4

Parameter	Unit	Value	Ref.
Current density	A m^{-2}	1440	84
Cell voltage	V	2.3	83
Faradaic efficiency	—	35% (C_2H_4) 56% (all C_{prod})	83
CO_2 utilisation degree	$mol_{C_2H_4}/mol_{CO\ in}$	100%	51
Carbon yield[a]	$mol_{C_2H_4}/mol_{CO\ reduced}$	63%	Calculated
Power density	kW m^{-2}	3.34	Calculated
Stack lifetime	h	40 000	35

[a] The carbon yield to product is calculated as the ratio between the FE towards C_2H_4, and the FE towards all carbon-products (C_{prod}, incl. C_2H_4).

Table 16 Investment costs for the tandem HT-LT CO_2 electrolysis process to produce C_2H_4

Parameter	Unit	Value	Ref.
Total HT CO_2 electrolysis and purification system (uninstalled costs)	€ per kW[a]	260	This study
Total LT CO electrolysis and purification system (uninstalled costs)	€ per kW	6000–12 700	This study
Tandem HT-LT CO_2 electrolysis plant to produce C_2H_4.(total investment costs)	€ per kW	12 300–25 700	This study

[a] The capacity of the HT system is adjusted to the capacity (in kW) of the LT system.

is used by the LT conversion step. In the HT step, 5.0–5.5 kg of CO_2 is converted into 3.2–3.3 kg CO, the latter is used in the LT step to produce 1 kg of C_2H_4 and some H_2 and ethanol as side-products. These steps together generate as a by-product 8.4–8.5 kg of O_2. The complete mass and energy balance for the tandem CO_2 to C_2H_4 process is shown in Table S9.†

For the tandem route, there will be two major components for the investment costs: the HT CO_2 to CO electrolyser (incl. the PSA unit), and the LT CO electrolyser to produce C_2H_4, with the downstream PSA unit. The method for estimating the investment costs is analogous to that for the rest of the routes, *i.e.* the HT step is based on data for HT solid oxide steam electrolysis and the LT step on PEM water electrolysis and both are corrected for the power density factors. The capacity of the HT electrolyser is adjusted to the required CO demand for the LT CO electrolyser. The total specific CAPEX for the two-step process is slightly higher in comparison to route 3, the single-step LT route to produce ethylene, and amounts to 12 300–25 700€ per kW (Table 16).

A summary of the design and material usage for each of the technologies used in the different routes is provided in Table S10 (see the ESI).†

3 Techno-economic analysis

Here, we report the results of our production cost assessment of the six routes. The routes consist of three LT electrochemical conversion routes that either produce CO, formic acid, or ethylene, two HT routes to produce CO or syngas, and one tandem approach (combination of HT and LT technology) to produce ethylene. The sensitivity analysis and cost projections up to 2050 are presented and discussed.

3.1 Investment costs

A more detailed description of the investment costs for the different routes is provided in the state-of-the-art sections (see above). In Fig. 21, we compare the cost breakdown of the base case total investment costs (CAPEX) for each of the routes for 1 MW scale plants. The LT conversion technology is currently significantly more expensive per kW of electricity input compared to the HT routes (4 and 5). This is also observed for the tandem process (route 6) in which the contribution of the first HT step (HT CO production system, dark green area) is barely noticeable (*ca.* 1% of the total CAPEX). The stack costs for LT systems are based on PEM technology for hydrogen production (see Table 3). For CO_2 reduction, the stack is operated at a lower power density, which results in significantly higher costs per kW electricity input. Next to relatively high specific stack costs, the presence of the CO_2 recovery loop, along with the purification unit for the end-product (PSA for gaseous products, and distillation for formic acid), represent a large contribution to the high total investment costs.

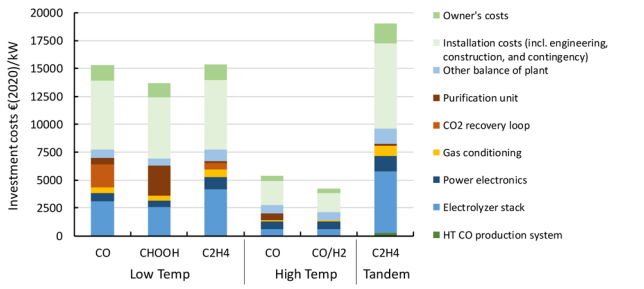

Fig. 21 Cost breakdown of the base case total investment costs for each of the six electrochemical conversion routes for a fixed 1 MW capacity. Note the strong uncertainty related to CAPEX assessment of early-stage technologies which have never been built and operated in a commercial environment.

The system and operating power density for our HT CO_2 reduction routes are fairly similar to those of HT steam electrolysis for hydrogen production. This allows us to base our cost calculations on steam electrolysis data, which is reported in more detail. For route 4, we add the costs of a PSA unit to separate CO from CO_2 of which the latter is recycled to the stack. For syngas production (route 5), we assume the synthesis gas that is produced is ready for use in, for instance, a methanol synthesis reactor, and does not require any further purification step. Such a step might appear necessary if the product gas is not directly suitable for follow-up chemical processes.

Our total investment costs cover nearly all project costs to build a CO_2 electrochemical conversion plant. Next to direct equipment costs, the installation and owner's costs are also included and represent roughly half of the total plant costs. In the refining and petrochemical industries, typically an installation factor of around 3–5 is used to acquire a rough estimate of the total project costs based on the costs for the main equipment.[85,86] If we only consider the electrolyser stack and power electronics as main equipment, our estimates correspond reasonably well with this factor. If other balance of plant costs, gas conditioning, and purification units (*e.g.*, PSA/CO_2 recovery loop) are included in the main equipment costs, our applied installation factor (~2) seems relatively low for a chemical process plant. We justify our choice by using a similar installation factor as applied for capital cost calculations for large electrolytic hydrogen production plants.[87]

In comparison to specific investment costs of other chemical processes, such as water electrolysis[38,86,88,89] or methanol synthesis,[90,91] the costs corresponding to electrochemical CO_2 conversion processes are relatively high, especially the LT routes. This can be expected of technologies at a low TRL because these do find themselves still at the start of their learning curve and significant cost reductions can be expected as soon as these technologies are further developed and scaled up. The effect of the investment costs on the levelized production costs is explained in the next section.

3.2 Levelized production costs

Current market prices of the products can provide a reasonable indication of the possible competitiveness of our routes. For bulk syngas and CO, it is difficult to estimate such a price because the market is non-existing. These gases are highly toxic and generally produced and directly converted into other products on site. To

approximate a fossil-based reference price, a figure between the price of natural gas and methanol is chosen, ranging in 2019 between 7 and 12€ per GJ.[92] To accommodate for recent volatility in natural gas and methanol prices,[93] we increased our high estimates by approximately 50%. Our reference price is, thus, fixed at 7–18€ per GJ or 0.07–0.18€ per kg CO or 0.17–0.43€ per kg syngas. As a specialty chemical in gas cylinders, CO sells at a price that is an order of magnitude higher. Formic acid is mainly produced through the reaction of methanol with CO to form methyl formate, which is subsequently hydrolysed. Market prices varied approximately from 130 to 150€ per GJ or 0.70–0.80€ per kg FA in early 2022.[94] Ethylene is typically produced *via* steam cracking of naphtha or natural gas liquids. The market price in the first quarter of 2022 varied between around 16 to 27€ per GJ or 0.70–1.30€ per kg C_2H_4.[95]

As described in the Methodology section (see the ESI†), our levelized production cost calculations rely on investment costs, operating and maintenance (O&M) costs (of which we separately specify the stack replacement costs), and feedstock costs (incl. electricity, CO_2, and H_2O). The total investments for each of the routes, as presented in the previous section, are annualized by multiplying with the capital recovery factor using a discount rate of 10% and a plant lifetime of 20 years. The annual O&M costs are a fixed percentage of the initial total investment costs. We average out the replacement costs for the stack as a separate annual O&M cost component. For the base case, costs for electricity are 40€ per MW h, for CO_2 50€ per t_{CO_2}, and for H_2O 1€ per t_{H_2O}. More information can be found in the ESI (*e.g.*, Table S1).†

Fig. 22 shows the results of the levelized cost calculations for our base case. From the figure, it is clear that the stack replacement, O&M and investment costs are driving the levelized costs of all products and routes.

For LT electrochemical CO_2 conversion, the levelized costs to produce CO amount to approximately 500€ per GJ or 5.1€ per kg (Fig. 22). Investment costs contribute more than 60%, O&M costs (incl. stack replacements) cover just above 30%, and the feedstocks, electricity and CO_2, together less than 10%. The investment costs dominate the LT CO production costs. This effect is typically exaggerated for low TRL technologies because several parameters (indirect investment costs and O&M cost components) are related to the main equipment costs.

Formic acid can be produced for almost 700€ per GJ or 3.7€ per kg (Fig. 22). The distribution of the costs over the different components is nearly identical to that of the LT CO production route. The costs per GJ of FA are slightly higher compared to those of CO. This can be explained by the lower energy efficiency of the formic acid production process with respect to CO production (resp. 26% *vs.* 40%). This difference in cost per GJ product becomes more apparent for C_2H_4 production for which the energy efficiency is only 16%. The lower the efficiency, the more capacity in kW is required to produce a GJ of product, next to additional expenses for electricity. Together this results for the direct process (route 3) in levelized costs of nearly 1270€ per GJ or 60€ per kg ethylene of which the feedstock costs (electricity, CO_2, and H_2O) only represent 6% in total, while the rest is for CAPEX (60%), O&M (20%), and stack replacement costs (14%). The tandem process (route 6), which is slightly less efficient and has higher CAPEX, is even more expensive than route 3 and costs amount to more than 1600€ per GJ or 76€ per kg ethylene. The ethylene production costs are approximately two orders of magnitude higher than our fossil reference price.

The HT processes benefit from relatively lower investment costs and higher energy efficiency. The levelized costs to produce CO are slightly below 200€ per GJ or 1.9€ per kg for route 4 (Fig. 22). Nearly a quarter of these costs come from the stack replacement costs, which are relatively high due to the low stack lifetime of only 8000 hours. Despite having an advantage in costs over the LT route (route 1), our fossil reference price is still at least ten times lower. Syngas production *via* HT route 5 results in levelized costs of around 80€ per GJ or 1.9€ per kg syngas. This route is currently the closest to its fossil reference of 7–18€ per GJ and may under specific conditions already be competitive.

3.3 Sensitivity analysis

The levelized production costs, as presented in the previous section, are our base case estimates. Most parameters are not fixed values and are better described as a range. To illustrate the dependence of the total production costs on a single parameter,

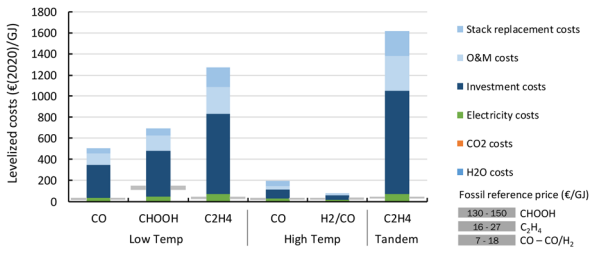

Fig. 22 Base case levelized production costs of different CO_2 electrochemical conversion routes. A breakdown of the costs is indicated by the coloured areas for each of the key cost components. Note the strong uncertainty related to CAPEX assessment of early stage technologies which have never been built and operated in a commercial environment. More details can be found in the enlarged diagrams in Fig. 25–30.

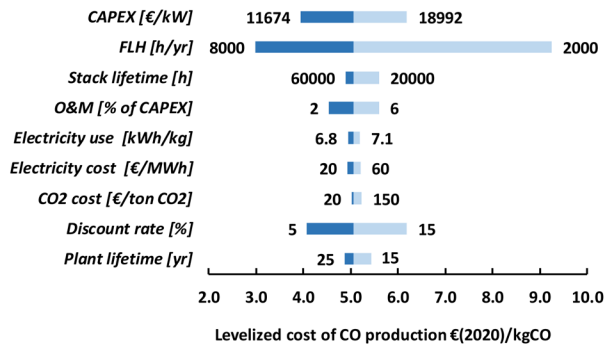

Fig. 23 Sensitivity analysis for route 1 – LT electrochemical conversion of CO_2 to CO. Nine parameters are varied to explore their effect on the current base-case levelized cost of CO production. The fossil reference CO price amounts to 0.07–0.18€ per kg_{CO}.

we have performed a sensitivity analysis for each of the routes. The low temperature routes, as well as the tandem route, rely mainly on CAPEX and, as a result, all parameters that are correlated to CAPEX have a substantial impact on the levelized production costs. This is shown for route 1 in Fig. 23. The uncertainty in current CAPEX estimates has a substantial impact on the range of levelized production costs. Our base case value of 5.1€ per kg of CO may reduce to approximately 4€ per kg for our optimistic CAPEX value or increase to more than 6€ per kg if the investment costs approach 19 000€ per kW. If the amount of full-load hours (FLH) is either doubled or halved compared to our base case of 4000 FLH, the installed capacity also doubles or halves. The production costs almost linearly follow this trend and at nearly full load (8000 FLH), the levelized CO production costs go down to 3.0€ per kg. Currently, in most countries the intermittency of renewable electricity supply results in boundary conditions for the operation of processes to produce renewable products to avoid the use of fossil-based electricity (see also Chapter 4). At some locations or in the future, to drive these processes for more than 4000 FLH seems possible, and, especially as long as CAPEX is a dominant cost factor, this may have a substantial impact on the levelized production costs. The stack lifetime is important to assess the costs associated with maintenance (*i.e.* stack replacement costs). Our base case value of 40 000 hours is based on PEM electrolyser stacks and improvements (*e.g.*, up to 60 000 hours) have a clear, but limited, positive effect on the production costs. A reduced stack lifetime (*e.g.*, down to 20 000 hours) has, however, a larger negative impact and achieving a certain level of stack lifetime, thus, seems an important development target. The O&M costs are a constant percentage of the CAPEX in our analysis and, as a consequence, their impact is high as long as the investment costs dominate the total production costs. Also, the discount rate directly affects the investment cost component and, because CAPEX is currently so high for LT routes, resembles an important parameter. The plant lifetime influences our CAPEX component in that it is used to calculate the capital recovery factor (ESI, eqn (2)†) and its impact on the production costs remains rather low if the lifetime is at least 20 years.

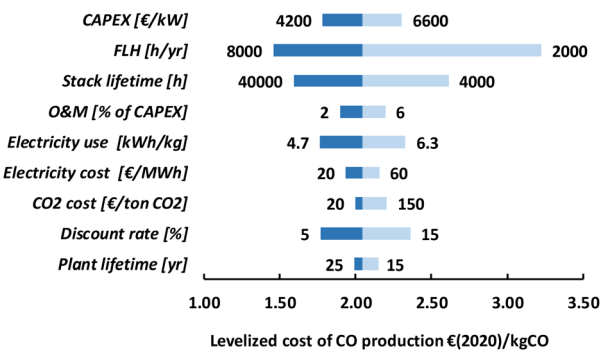

Fig. 24 Sensitivity analysis for route 4 – HT electrochemical conversion of CO_2 to CO. Nine parameters are varied to explore their effect on the current levelized cost of CO production. The fossil reference CO price amounts to 0.07–0.18€ per kg_{CO}.

The electricity use and costs are at this stage not so relevant for the levelized CO production costs. Even electricity costs as low as 20€ per MW h do not lead to a substantial cost reduction. The same holds for CO_2 costs because varying those from 20 to 150€ per t_{CO_2} only results in a difference in production costs of 0.2€ per kg_{CO}, which is relatively a minimal impact. For routes 2, 3, and 6, the sensitivity analysis tells a nearly identical story as for route 1 and we refer to the ESI for more information (Fig. S6, S7, and S9).†

The specific investment costs for our two HT routes are significantly lower compared to the LT routes and the results of our sensitivity analysis for route 4 are presented in Fig. 24 (see Fig. S8 in the ESI for route 5).† When CAPEX is less dominant, the role of other parameters becomes more apparent. Our variation in electricity use has for HT route 4, for instance, a similar influence on the levelized cost of CO production as has our investment costs range. The explored range in feedstock costs (electricity and CO_2) provides a more than 10% difference in levelized costs, which is much higher compared to the LT route (<5%).

For all routes, investment costs are an important component as can be expected for low TRL technologies. It is however likely that these costs can be reduced substantially during scale-up and deployment. In the next section, we explore how such cost reductions may influence the competitivity of our routes in the future.

3.4 Cost projections

As indicated in the previous sections, the current costs to electrochemically convert CO_2 into products are high compared to fossil-based alternatives. The costs may be reduced substantially thanks to, for instance, learning-by-searching, learning-by-doing, economies-of-scale, and lower material costs. We apply a learning curve analysis on the CAPEX component of our six conversion routes to explore how several of these phenomena affect the future investment costs. The insights from these learning curves are used to project the production costs for 2030, 2040, and 2050, taking into account several performance improvements in the electrochemical conversion processes.

3.4.1 Investment cost learning curves and future production costs. A technology learning curve is generally based on empirical data of observed cost reductions in the past (see also ESI, section 1.5†). The curve generally resembles a declining straight line if costs are plotted against the cumulative installed capacity (CIC) on two logarithmic axes. By extrapolation of a historical learning curve, cost reductions can be projected if the cumulative installed capacity is increased. The learning rate (LR) for various energy technologies ranges typically between 10 and 30%.[96,97] As an example, the LR for solar PV amounts to 24%,98 while an average LR of 12% is reported for onshore wind.[99] To assess new technology, for which empirical data are often lacking, an estimate can be made of the learning curve based on the current technology status and analysis of comparable technology. Here, we assess two key systems: low temperature CO_2 electrolyser plants and high temperature CO_2 electrolyser plants.

Table 17 Learning curve parameters for electrochemical conversion technology. Onshore wind and solar PV are included for reference

Study	Technology	CIC	LR (applied)	Year(s)
This study	LT CO_2 electroconversion	45 GW (2020)	15 ± 5	2020–2050
This study	HT CO_2 electroconversion	0.5 GW (2020)	20 ± 5	2020–2050
Rubin *et al.* 2015 (ref. 98)	Onshore wind	837 GW (2021)[105]	12	1979–2010
ITRPV 2022 (ref. 97)	Solar PV	972 GW (2021)	24	1976–2021
Schoots *et al.* 2008 (ref. 99)	LT electrolysis	15 GW (2006)	18 ± 13	1956–2006
Schmidt *et al.* 2017 (ref. 100)	LT electrolysis	20 GW (2014)	18 ± 6	1956–2014
Krishnan *et al.* 2020 (ref. 101)	LT electrolysis	20 GW (2016)	16 ± 6	1956–2016
Schoots *et al.* 2010 (ref. 102)	PEMFC	0.3 GW (2008)	21 ± 4	1995–2006
Rivera-Tinoco *et al.* 2012 (ref. 104)	SOFC	0.05 GW (2009)	35	1986–2009
Wei *et al.* 2017 (ref. 103)	PEMFC	0.8 GW (2015)	18	2005–2015
Wei *et al.* 2017 (ref. 103)	SOFC	0.1 GW (2015)	~0	2001–2015
Detz *et al.* 2018 (ref. 89)	LT electrolysis (AE)	21 GW (2015)	18	2015–2050
Detz *et al.* 2018 (ref. 89)	LT electrolysis (PEM)	0.8 GW (2015, PEMFC)	21 (PEMFC)	2015–2050
Detz *et al.* 2018 (ref. 89)	HT electrolysis	0.2 GW (2015, SOFC)	27 (SOFC)	2015–2050
Bohm *et al.* 2019 (ref. 39)	LT electrolysis (AE)	20 GW (2015)	18	
Bohm *et al.* 2019 (ref. 39)	LT electrolysis (PEM)	1 GW (2015)	18	
Bohm *et al.* 2019 (ref. 39)	HT electrolysis	0.1 GW (2015)	18	
Detz & Weeda 2022 (ref. 88)	Electrolysis	20 GW (2020)	9–20	2020–2050
IEA, 2021 (ref. 27)	Electrolysis	0.3 GW (2020)	15 (stack)	2020–2050
Calculated in this study	Chlor-alkali	40 GW (2020)		
Calculated in this study	LT electrolysis	3.3 GW (2020)		

Low temperature systems to convert CO_2 into products are still at the pilot stage (kW scale systems) and current installed capacity is low (<MW). High temperature processes are slightly further in TRL but their cumulative installed capacity is also low (few MW) because the largest projects are currently developing MW systems. To project their learning curves, we base our initial cumulative experience and learning rate on that of comparable technology. For LT CO_2 conversion, the technology is fairly similar to the chlor-alkali electrolytic process. The electrolyser stack, as well as the power electronics and other balance-of-plant equipment, are basically the same. Some pre-treatment and purification steps differ because these have to deal with other starting materials and products. The same manufacturers supply equipment for the chlor-alkali, the electrolytic hydrogen, as well as the electrochemical CO_2 conversion industry. This justifies the use of existing experience and learning curve data of electrolytic production of chlor-alkali and hydrogen. To our knowledge, no learning curve has been reported for chlor-alkali investment costs. For electrolytic hydrogen production, several contributions report about a historical learning curve for electrolysers,[100–102] and projections of cost reductions based on a learning curve.[27,39,88,89] The results and assumptions of these studies have been summarized in Table 17. An important parameter for our projections is the initial cumulative installed capacity on which we base the existing experience because this value determines the amount of novel capacity that has to be installed before another doubling in cumulative capacity is reached. The value varies slightly among the studies but in each case seems to be based on the total capacity of both electrolytic chlor-alkali and hydrogen production systems. For our analysis, we assume that all experience gained in the chlor-alkali, water electrolysis, and PEM fuel cell industries is both part of the historical learning but also for future learning effects. This means that the total cumulative installed capacity for low temperature electrochemical conversion technology represents a substantially higher figure than used in most previous studies. The total production capacity of the chlor-alkali industry is currently

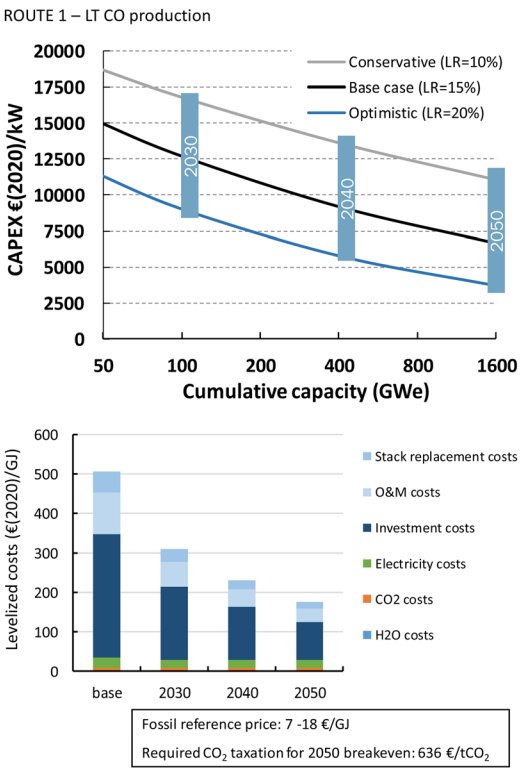

Fig. 25 Route 1 cost projections of the CAPEX (top) and the base case levelized CO production costs (bottom) for LT electrochemical CO_2 conversion to carbon monoxide. The CIC of LT electroconversion processes in 2020 is 45 GW_e.

Table 18 Considered efficiency improvements for the six conversion routes[a]

Route	Parameter	2020	2050
1	Energy efficiency	40%	56%
2	Energy efficiency	26%	47%
3	Energy efficiency	16%	39%
4	Energy efficiency	50%	90%
5	Energy efficiency	82%	86%
6	Energy efficiency	16%	32%

[a] For LT technology, these improvements come mainly from an improved cell voltage in 2030.[28] For HT technology, own calculations indicate a possible reduction of the energy use for the balance-of-plant equipment, mainly for route 4.

around 22 GW and cumulatively approximately 40 GW of capacity (including replacements) has been installed over time. Together with water electrolysis and PEMFC systems, we arrive at an initial CIC of 45 GW for LT electroconversion routes. Historical learning curves for LT electrochemical devices have been reported for water electrolysis and PEM fuel cells (PEMFC).[99–101,103,104] The learning rates vary between 16 and 21%. Many of these learning rates are based on the (manufacturing) costs of the system and do not include other costs that contribute to the construction of an entire chemical plant. Several of these other components are more mature as the electrolyser stack and benefit less from learning effects. We therefore apply to the total investment costs a conservative LR range of 10–20% with 15% as base case value.

HT electroconversion systems differ substantially from their LT counterparts. The stacks contain no liquids and consist of solid ceramic materials, while the balance-of-plant equipment has to deal with gases and steam throughput and high process temperatures. We therefore select our starting point based on both SOFC and SOEC technology. The total CIC of such systems is estimated to be approximately 0.5 GW, mainly SOFCs. As far as we know, two learning curve analyses have been reported for SOFC technology, but the learning rates vary significantly from 0 to 35%.[103,106] Such a broad range is illustrative of the high uncertainty with which assessment of technologies at an early development stage is typically accompanied. For instance, a lack of markets and competition can reduce the urgency for a manufacturer to produce and sell cheaper systems. We apply for our HT routes a slightly higher LR range compared to the LT systems, of 15–25%, with 20% as the base case value.

The projected learning curves for all our routes are depicted in Fig. 25 to 30. For LT CO production route 1, the total investment costs reduce from currently approximately 11 700–19 000€ per kW_{el} to 3700–11 000€ per kW_{el} after around five

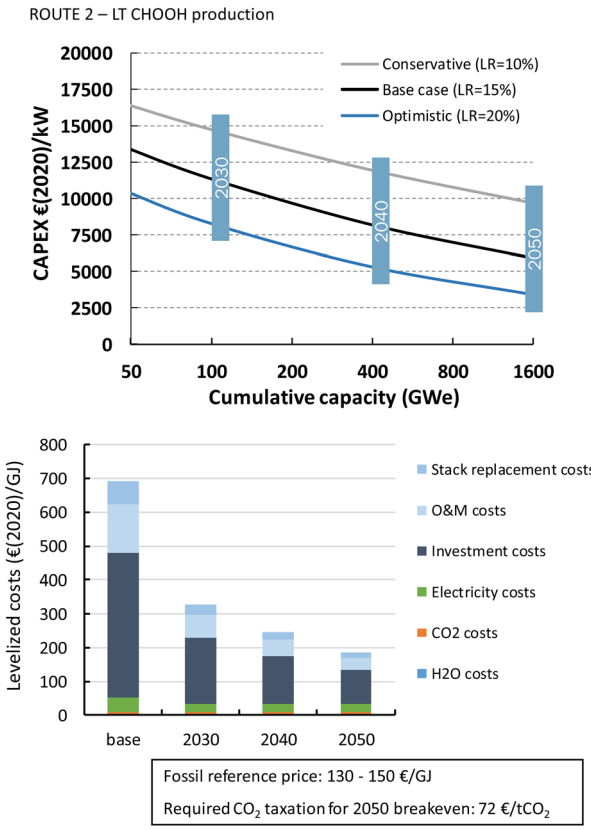

Fig. 26 Route 2 cost projections of the CAPEX (top) and the base case levelized FA production costs (bottom) for LT electrochemical CO_2 conversion to formic acid. The CIC of LT electroconversion processes in 2020 is 45 GW_e.

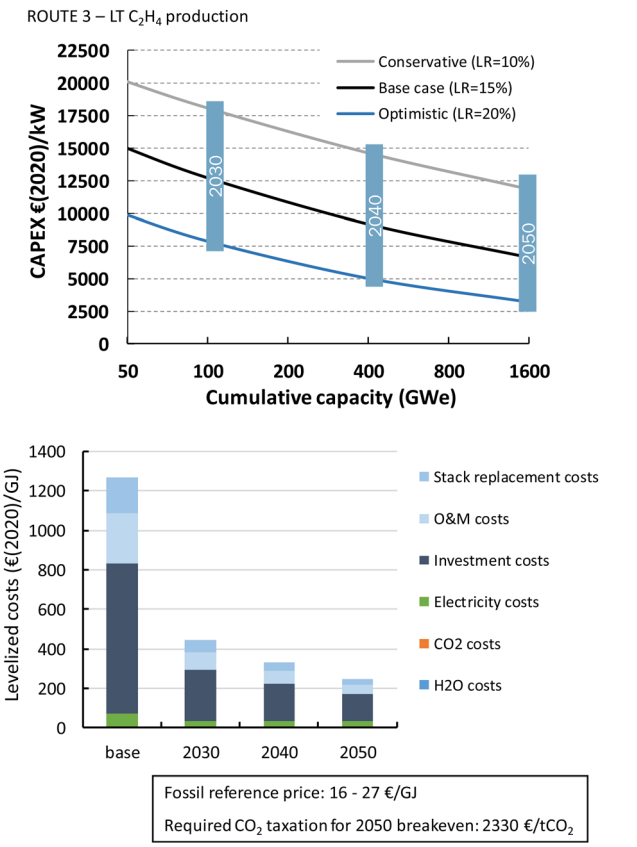

Fig. 27 Route 3 cost projections of the CAPEX (top) and the base case levelized C_2H_4 production costs (bottom) for LT electrochemical CO_2 conversion to ethylene. The CIC of LT electroconversion processes in 2020 is 45 GW_e.

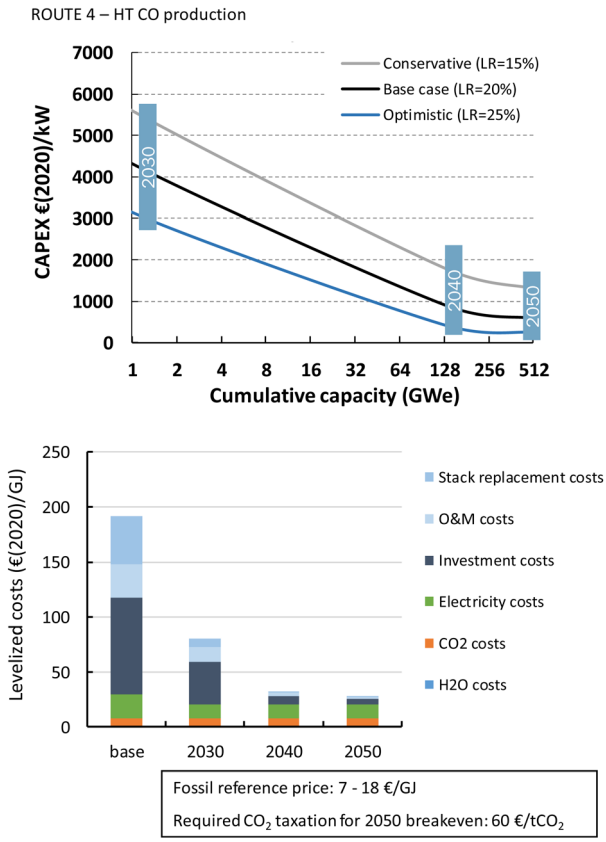

Fig. 28 Route 4 cost projections of the CAPEX (top) and the base case levelized CO production costs (bottom) for HT electrochemical CO_2 conversion to carbon monoxide. The CIC of HT electroconversion processes in 2020 is 0.5 GW_e.

doublings in CIC (Fig. 25). If 1.6 TW of LT electrochemical devices has been installed in 2050, our base case projection amounts to 6600€ per kW_{el}, which is nearly a 60% reduction in CAPEX compared to 2020. This cost reduction is through our applied learning curve induced by multiple factors, such as economies-of-scale, manufacturing improvements, and process optimization, among others. We indicate that our specific CAPEX in kW_{el} input and improvements in the power density of the process have a tremendous impact on the output per kW_{el}. This effect has not been investigated separately but the indirect consequence of our analysis implies that it is not straightforward that CAPEX scales linearly down with increasing power density. In other words, we assume that raising the power density goes paired with an increase in CAPEX. Notably, if in reality the power density can be improved without affecting the investment costs, costs may reduce faster as projected here. From the levelized production costs calculations (see above), it became clear that CAPEX resembles the key cost component for our routes. Lower investment costs, thus, have a substantial impact on the levelized production costs, which in our base case scenario reduce from 2020 to 2050 by nearly 65% to 175€ per GJ (1.75€ per kg). A small contribution to the observed cost reduction comes from improvements in energy efficiency (Table 18). In comparison to our fossil benchmark of below 18€ per GJ, these costs are still high. Only with a CO_2 tax of at least more than 600€ per t_{CO_2}, the production costs of route 1 can reach a breakeven point with the fossil reference price. On the specialty chemicals market with prices around 3€ per kg,[107] the LT CO production route might become competitive already in 2030, even without CO_2 taxation.

The investment cost projection for LT formic acid production (route 2) follows a similar pattern to that for route 1. CAPEX reduces from currently 10 700–16 700€ per kW_{el} to 3400–9700€ per kW_{el} going up in CIC to 1600 GW_e (Fig. 26). This has a positive effect on the projected levelized cost as these go down from nearly 700€ per GJ today, to below 200€ per GJ in 2050. Such a cost level is already close to our fossil reference price and, for breakeven, a CO_2 taxation of approximately 70€ per t_{CO_2} should be sufficient.

The investment cost projection for LT ethylene production (route 3) reduced from an initial 10 700–16 700€/ per W_{el} to 3400–9700€ per kW_{el} for a CIC of 1600 GW_e (Fig. 27). The positive effect of a lower CAPEX on the levelized production costs of ethylene is further enhanced by a higher conversion and energy efficiency of the process. Together these developments result in a cost decline of 80% compared to our current base case costs by 2050. The levelized costs of 250€ per GJ ethylene in 2050 are a factor of ten higher than our fossil

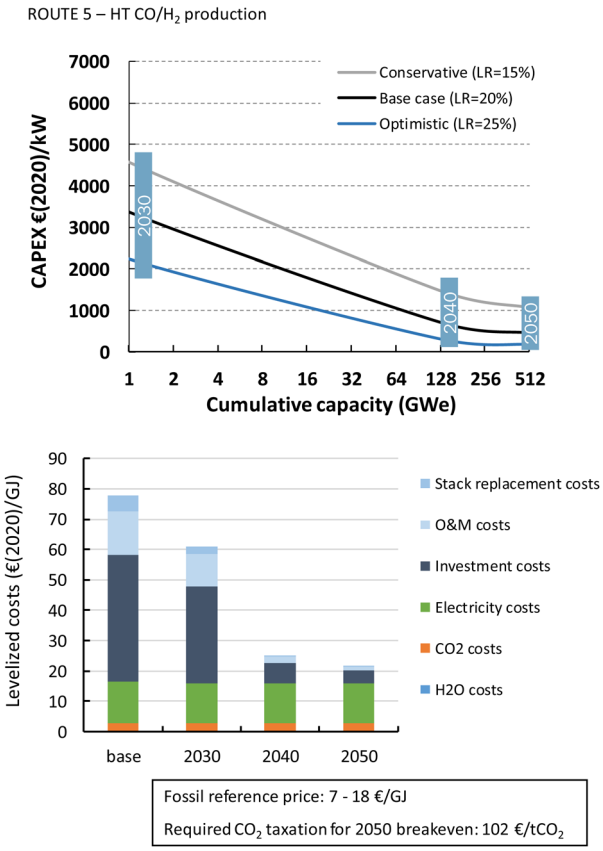

Fig. 29 Route 5 cost projections of the CAPEX (top) and the base case levelized syngas production costs (bottom) for HT electrochemical CO_2 conversion to syngas. The CIC of HT electroconversion processes in 2020 is 0.5 GW_e.

reference price. Only with a very high CO_2 tax of more than 2300€ per t_{CO_2}, which may be unrealistic, a cost-breakeven point can be reached.

The specific investment costs for HT CO_2 electrochemical conversion (routes 4 and 5) are significantly lower in comparison to LT routes. For CO production, CAPEX ranges currently between 4200 and 6600€ per kW_{el}, which is already close to the 2050 projections for our LT routes. Descending its learning curve, the costs go down rapidly thanks to the relatively high LR of 20% for the base case compared to 15% for our LT routes. We project that around 0.5 TW of cumulative capacity will be installed in 2050. As mentioned, this value includes the installed capacity of solid oxide water electrolysers and fuel cells. In such a scenario, the investment costs reduce to 240–1300€ per kW_{el} (Fig. 28). This CAPEX reduction, together with improvements in energy efficiency and prolonged stack lifetime, results in levelized production costs for CO of 28€ per GJ or 0.28€ per kg in 2050. This is close to the fossil reference price of 7–18€ per GJ and a CO_2 tax of 60€ per t_{CO_2} would already induce a point of breakeven.

The investment costs for HT syngas production currently amount to 3000–5400€ per kW_{el} and our projection indicates that costs may go down to 170–1060€ per kW_{el} (Fig. 29). This is the main driver for a significant reduction of the levelized costs to produce syngas *via* this route towards 2050. In 2050, the dominant cost component is the electricity costs, which represent nearly 60% of the total production costs of 22€ per GJ or 0.53€ per kg. To become competitive with the fossil reference price of 7–18€ per GJ, a CO_2 taxation of at least 100€ per t_{CO_2} would be required.

In the tandem process (route 6), first CO_2 is converted by a HT system into CO, which is the feed for a LT electrolyser in which ethylene is produced. The current investment costs heavily rely on the costs of the LT system (>95%). This justifies the application of the learning curve parameters for the LT technology to the total investment costs. Our learning curve indicates that costs go down from 12 300–25 700€ per kW_{el} now to 5300–11 100€ per kW_{el} in 2050 (Fig. 30). For our base case in 2050, this means that investment costs still dominate the ethylene production costs, which reduce by more than a factor 4 to 374€ per GJ or nearly 18€ per kg ethylene. In our projections, any improvements in selectivity and efficiency of the process are excluded. These developments would further reduce production costs because of lower energy usage and potentially less required capacity to produce a certain amount of ethylene. Compared to the fossil reference price of 16–27€ per GJ, such a cost is very high and only with exceptionally high CO_2 pricing (>3600€ per t_{CO_2}) a point of breakeven can be reached.

4 Greenhouse gas emission performance

The prospect of novel technologies to produce fuels and chemicals depends largely on their competitiveness with conventional pathways. We indicated in the previous chapters that if learning-by-doing proceeds as expected, some CO_2 electrochemical conversion routes may become economically competitive with alternative approaches based on fossil resources. Notably, this only seems possible if sufficient CO_2 taxation is in play, ranging from 60 to more than an unrealistically high 3600€ per t_{CO_2}. It will be important that the GHG emissions associated with our routes are significantly lower compared to their fossil reference. Here, we calculate the CO_2 emissions for each of the six routes by comparing the indirect emissions from electricity use of both the CO_2 capture technology as well as the electroconversion (and purification) technology (Fig. 31). This can serve as a best-case orientation because it doesn't consider other emissions, for

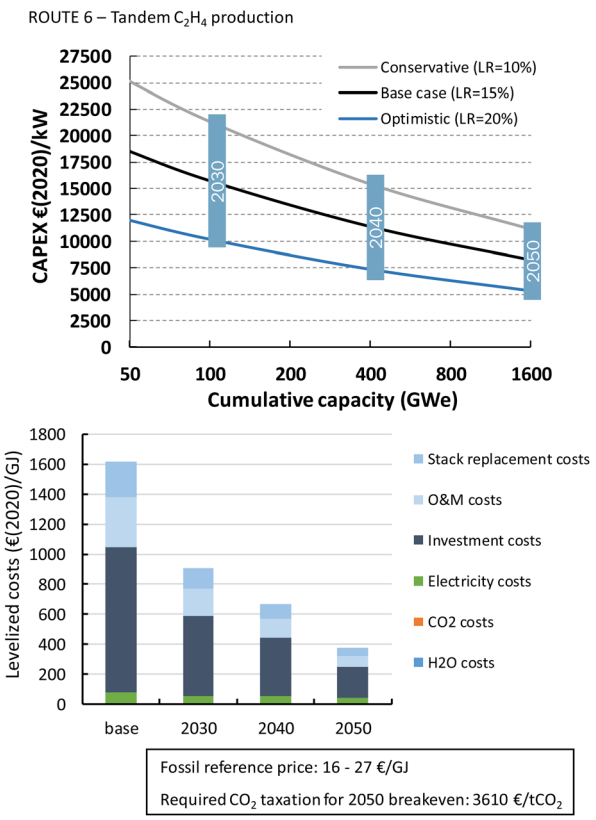

Fig. 30 Route 6 cost projections of the CAPEX (top) and the base case levelized C_2H_4 production costs (bottom) for Tandem electrochemical CO_2 conversion to ethylene. The CIC of LT electroconversion processes in 2020 is 45 GW_e.

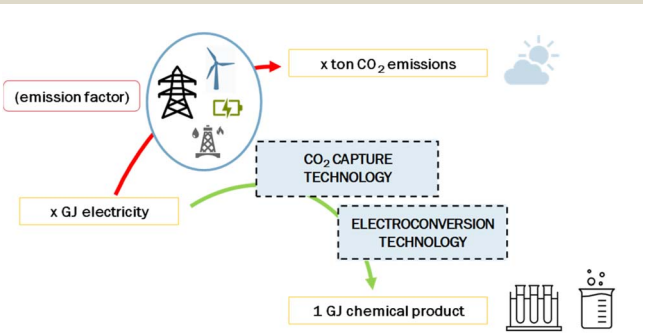

Fig. 31 Calculated CO_2 emissions associated with electrochemical conversion routes.

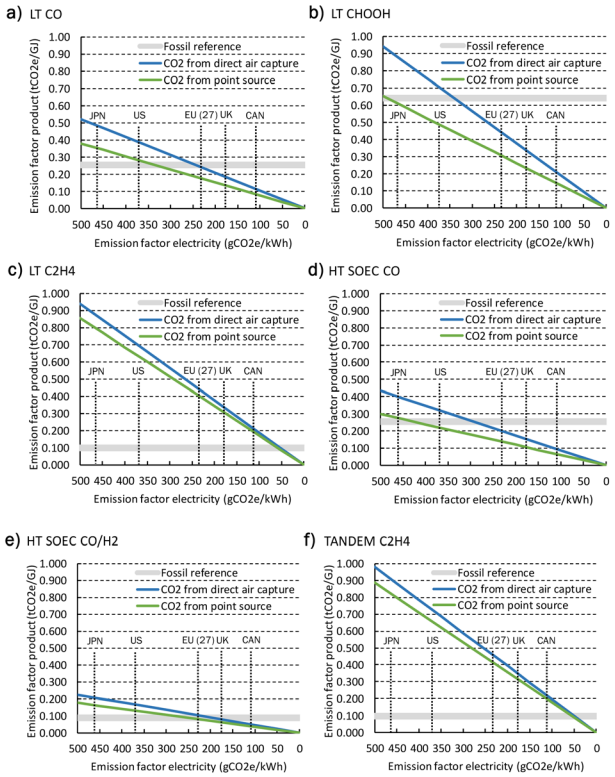

Fig. 32 Emissions from electricity use for the six electrochemical CO_2 conversion routes. The vertical dotted lines indicate the emission factor of the grid in a specific country/region in 2020.

instance from construction or equipment manufacturing. The emission factor of the electricity supply clearly affects the total emissions of the route (Fig. 32). Our routes start from CO_2 as feedstock, without taking into account (for the cost analysis) the origin of this CO_2. To supply CO_2 as a feedstock for our routes, energy is required for the capture, which can be either from a point source or from the air.

To indicate the difference in energy regarding point source capture and DAC, we show both scenarios, *i.e.*, the emission factor of the product based on either point source capture (green lines) or DAC (blue lines). The energy use of point source capture depends on the type of point source and gas stream and, thus, varies significantly. We take a value (0.3 MW h per t_{CO_2}) at the lower side of the reported figures and assume that this energy can be supplied as electricity, either direct or *via* electric heating.[108,109] For DAC, we use similar assumptions, but the electricity use is determined to be at the high end of the reported range (2.0 MW h per t_{CO_2}).[110] By this, we cover more or less the entire range of emissions related to the electricity use for our CO_2 supply. The results are compared with the emissions related to the fossil reference pathway, which is based on average 100 year global warming potential values from the SimaPro database. In Fig. 32, the emission factor of the products of all routes (routes 1–6: a–f) has been displayed *versus* the emission factor of the electricity that is used for the process.

The LT route to produce CO can achieve similar emissions as the fossil reference when the emission factor of the grid is less than approximately 350 $g_{CO_2}e$ per kW h, which is currently the case in several countries, such as the United Kingdom (UK), Canada (CAN), and in the European Union (EU). To become a meaningful route to produce renewable fuels and chemicals, the emission factor of the products should, however, be significantly lower in comparison to fossil-based alternatives. European regulation for instance states that "the greenhouse gas emissions savings from the use of renewable liquid and gaseous transport fuels of non-biological origin (RFNBO's) shall be at least 70%".[111] To reach such a level of avoided emissions, the grid emission factor should be below 100 $g_{CO_2}e$ per kW h for route 1. For formic acid production (route 2), the emission factor of the fossil reference is rather high and breakeven emissions can be realized with a grid emission of 500 $g_{CO_2}e$ per kW h, while a 70% reduction is realized with electricity that is generated with emissions of maximal 150 $g_{CO_2}e$ per kW h. In several countries, thanks to an increasing share of renewable electricity supply, the average grid emission factor is already approaching such a value and would thus afford the electrochemical production of these products at full annual capacity. The levelized costs would reduce from our base case value of 3.7€ per kg for 4000 FLH to 2.2€ per kg for 8000 FLH. A totally different situation occurs for production routes 3 and 6 because the fossil reference emissions for ethylene production are relatively low and the electricity use of the electrochemical process is high. Only with a very low grid emission factor of around 50 $g_{CO_2}e$ per kW h, a product emission factor is obtained that is similar to the fossil reference. A >70% reduction target is within reach, but the grid emission factor should be close to zero.

The HT route 4 to produce CO is more efficient than the LT alternative and requires less electricity usage. The emission factor of the grid can be nearly 450 $g_{CO_2}e$ per kW h for this route based on point source CO_2 to achieve an emission breakeven point with the fossil reference. To realize >70% GHG savings, the difference between routes 1 and 4 becomes smaller in absolute terms and emissions from the grid may amount to 125 $g_{CO_2}e$ per kW h or 25 $g_{CO_2}e$ per kW h more than for route 1. Syngas contains less carbon per GJ of product compared to pure CO and its associated emission factor is analogously lower, also for the fossil reference. With grid emissions below 250 $g_{CO_2}e$ per kW h, the electrochemical pathway can compete in emissions with the fossil-based alternative. From around 70 $g_{CO_2}e$ per kW h and lower, substantial GHG savings (>70%) can be reached, purely based on the electricity use of the process. Background emissions throughout the entire supply chains and other environmental aspects are not (fully) analysed and may have an impact on our preliminary conclusions on the competitivity of these routes with fossil reference pathways. A full life-cycle assessment can provide more detailed insights into these aspects but is not part of this study.

5 Knowledge gaps and research directions

Here, we discuss the challenges and knowledge gaps that we identified in our study. We also proffer recommendations for

further research. Below we list specific technical challenges to be addressed for each technology and for the processes in general.

5.1 Low-temperature electrochemical CO_2 conversion routes

5.1.1 Uncertainty whether the roadmap for the future process performance indicators for the 2020–2030 decade is to be achieved. The routes to electrochemically produce CO and HCOOH show already high performance in terms of selectivity, cell voltage and current density, given their low electron exchange number. For more complex molecules with a higher number of electrons exchanged, such as C_2H_4, it is uncertain that the outlined projections of process parameters for CO and FA will hold true, especially for high faradaic efficiency and current density. Important challenges in LT CO_2 electrolysis technology development need to be overcome to realise the stipulated roadmap. The most important one is to ensure long-term stable operation (>10 000 h) at high current densities and efficiencies, and low cell voltage. To achieve this, also the problems of carbonate precipitation at the cathode should be solved (as stated by Küngas, 2020 and Stephens *et al.*, 2022).[30,112]. Also, the novel LT CO electroconversion from the tandem route (route 6) is gaining increasing attention amongst researchers, and the efficiency and selectivity are expected to improve with catalyst, electrode and material development. However, it is uncertain whether LT CO electroconversion will reach the same performance as the projected LT CO_2 electrolysis goals for the next decade postulated in the roadmap by Nørskov *et al.*[28]

5.1.2 Costly purification unit for the HCOOH case. From Fig. 21, it is clear that the chosen purification strategy to produce a concentrated aqueous FA stream (85 wt%) has a decisive contribution to the total investment costs. This is especially relevant in future scenarios for electrolysis stacks with higher productivity, entailing a required higher production capacity in the downstream purification train. It is of paramount importance to highlight the necessity of selecting an energy and cost-efficient purification strategy for any LT CO_2 electrolysis product, and more importantly, for liquid products. Alternatives to the selected hybrid-extraction distillation system can already be found in the literature, as for instance a pervaporation-driven process with potential low capital and operational expenses.[113]

5.1.3 LT CO_2 electrolyser lifetime. The presumed lifetime for LT CO_2 electrolysers for the economic analysis has been taken from the current process indicators for water PEM electrolysis (see Table 3). This figure can also be understood as a performance target to be achieved for LT CO_2 electrolysis, as it is for the future scenario projected for 2030 (see Fig. 6).[28] Lifetime is one of the most influential aspects for the economics of an electrolyser stack. It is the maximal operational time for a stack before it needs to be replaced by another one due to excessive performance loss (lower current, higher energy consumption). Ample research efforts have been dedicated to studying and understanding the phenomena that dictate the durability and long-term stability of LT CO_2 electrolysis processes, such as membrane degradation, water management in the GDE, and electrocatalyst stability.[111]

The best state-of-the-art lifetime data for LT CO_2 electrolysis (for CO production) lifetime are *ca.* 5000 h at low current densities (500 A m^{-2}) and small scale (10 cm^2).[30] It is therefore important to understand that the LT CO_2 electrolysis process is a technology under development, and a special R&D emphasis on ensuring long-term stability at high current densities (5000–10 000 A m^{-2}) is critical to make this concept industrially feasible. Kibria *et al.* stated that the necessary lifetime to obtain a feasible business case for LT CO_2 electrolysis should likely be higher than 80 000 h.[114]

5.1.4 CO_2 crossover towards the anode and associated costs for CO_2 recovery. The LT CO_2 electrolysis technology is characterised by the net loss of part of the CO_2 feedstock in the form of (bi)carbonates, migrated towards the anode side of the cell, as earlier explained.[115] The crossed-over CO_2 has to be reclaimed from the O_2-containing stream from the anode, with high associated capital (see Fig. 21) and operational costs. The chosen CO_2 reclaiming process is based on an energy-intensive DAC technology that can work with O_2-rich inlets, and potential new solutions can be applied for the separation of CO_2 from this stream. In the literature, several approaches have been proposed to specifically tackle the CO_2 crossover challenge for LT electrolysis. Kim *et al.* suggested a similar solution to the LT CO_2 to HCOOH route, with an acidic middle compartment that will strip the CO_2 from the bicarbonate anions, avoiding the mixing with O_2 in the anodic side.[116] Xie *et al.* proposed an alternative anodic reaction with a liquid product that will permit to strip of a pure CO_2 stream in the anode side.[117] From plasma-based processes for CO_2 conversion to CO, a promising CO_2–CO–O_2 separation technology has been reported using zeolites in a PSA process that can be applicable for the crossed over CO_2 towards the anode.[118]

5.1.5 Need for a CO_2/H_2 separation process in the LT route for HCOOH. Assuming that H_2 is only a by-product in the LT HCOOH process (route 2), it will accumulate in the cathode gas loop if not (partly) removed (with the associated loss of CO_2). A H_2/CO_2 separation process needs to be implemented in case the efficiency of the CO_2 to HCOOH reaction is not 100% (to be achieved by 2030 (ref. 28)). Industrially available technology using palladium-based membranes can be adopted for this application, normally used for H_2 purification for CO_2-containing streams.[119]

5.1.6 Role of the anodic reaction in the economic feasibility of CO_2 electroreduction. The chosen anodic reaction for all proposed routes is water oxidation producing O_2. For the LT area, this reaction is chosen because it is non-limiting for the cathodic CO_2 reduction reaction, despite being an energy-intensive reaction (high anodic overpotential) and O_2 being difficult to valorise economically (barely \$24–40 per t_{O_2}).[120] Several authors have already pointed out the potential of the anodic oxidation reaction for alternative products or applications, like product upgrade or wastewater treatment.[121] Pérez-Gallent *et al.* demonstrated that the coupling of 1,2-propanediol oxidation to lactic acid with CO_2 reduction to CO effectively doubles the product value per unit of electrical energy that is

used by the electrolyser (compared to the O_2 co-production system).[122]

By selecting a sensible anodic product that can easily be assimilated by the CCU value chain, the economic feasibility drastically improves.[119,123] An example of this strategy is the electrochemical co-production of CO and Cl_2 in equimolar amounts, the combination of which makes the precursor mixture for phosgene, a key intermediate for plastic and rubber manufacturing.[124] Also other chemicals, such as glycerol, can be oxidized at the anode to reduce the energy consumption and increase the product value.[125] Despite its potential economic advantages, the implementation of alternative anodic reactions to the OER is less pursued due to the: (1) low cost of water as reactant for the OER; (2) simplicity of disposing O_2 to the atmosphere instead of implementing costly purification strategies for the alternative anodic product; and (3) compatibility of the OER with intended CO_2 reduction reaction systems.[126]

5.2 High-temperature electrochemical CO_2 conversion routes

5.2.1 Stack and system level research directions. On the solid oxide stack, several research directions are aimed at lowering costs. The FCH program aims at lowering the stack cost to below 150 EUR per kW.[127] Other research studies aim at reducing the dependence on raw materials at the cell level (cobalt, nickel, and yttrium). Upscaling beyond the MW level requires optimal system design for better heat management.[128] Lowering stack replacement costs by improving the stack lifetime *via* reduction of degradation at the cell level may further reduce production costs.[30]

5.2.2 Separation of CO from CO_2/CO stream. Currently, there is not enough data regarding separation technologies for a CO/CO_2 stream. As shown in Fig. 14, the use of a PSA unit to obtain a high purity CO stream is depicted in the block diagram.[56] However, data regarding yield, purity, and costs of such PSA units are not publicly available.

5.3 General aspects for electrochemical CO_2 conversion routes

5.3.1 Required purity of CO. In today's conventional process, CO is produced as 'captive' CO and used on-site with a bespoke composition for the subsequent process. It is not straightforward to compare the electrochemical products with a reference in terms of levelized production cost, purity, and associated CO_2 emission. Higher purity can be achieved with further downstream processing at higher cost and *vice versa*. CO costs and emissions also strongly depend on the reference technology: coal gasification or steam methane reforming combined with a water gas shift reaction and gas purification.

5.3.2 Required purity and composition of syngas. Syngas is typically produced as captive syngas and used on-site for different applications such as methanol production or Fischer–Tropsch synthesis ($H_2 : CO = 2 : 1$). The application in which the syngas is applied determines the required composition of produced syngas from the SOEC system outlet. Hence, the ratio of steam and CO_2 feedstock must be changed to obtain a syngas with a specified CO/H_2 ratio. Moreover, in the case of syngas, separation technology costs for CO/CO_2/H_2 depend strongly on the intended end-use of the product.

5.3.3 Required CO_2 purity and role of impurities for CO_2 electroreduction. Purity requirements of the CO_2 feed are usually considered out-of-scope in research projects and not reported in published research. Also in our study, we leave out the type of CO_2 supply to the electrochemical unit. Different sources of CO_2 may contain different levels of impurities and require different degrees of purification. The role of impurities and undesirable contaminants in the inlet CO_2 gas stream in the electrolysis operation has not yet received enough attention amongst researchers, even though these trace components can have significant consequences for the stability and lifetime of the electrochemical unit. The presence of impurities such as nitrogen oxides, or sulphur-derived compounds can lead to severe catalyst deactivation.[129] NO_x compounds can lead to temporary catalyst deactivation because the active metal catalyst can be regenerated *in situ* with pure CO_2 streams.[130] Other contaminants, such as H_2S and SO_2, can irreversibly change the catalyst morphology and render the metal catalyst ineffective for CO_2 conversion, *e.g.* for copper-based systems.[131] These impurities are commonly found in CO_2 streams coming from, for instance, cement production and biomass conversion, which would require solutions to remove these trace components prior to considering the recovered CO_2 for CCU options. This will affect both the costs of the purification unit and the associated energy consumption.

5.3.4 From uninstalled cost to total plant cost. As most of the discussed technologies are at low and medium TRL, reported costs usually focus on stack costs. Real life total plant costs are yet unknown. Hence, total plant costs are estimated based on assumptions for balance-of-plant costs and using installation factors based on comparable technologies. These assumptions introduce uncertainties in the assessment of the total CAPEX. CAPEX estimates become more accurate as soon as first-of-a-kind projects are realized.

5.3.5 Need for total value chain pilot and demonstration projects. A general issue with all investigated pathways is that the research is usually limited to cell-level and stack-level research. Pilot and demonstration projects in which the entire product chain from industrial CO_2 stream to final product is demonstrated are needed to more accurately determine CAPEX and O&M costs in an industrial environment.

5.3.6 Integration in existing chemical clusters. A general research question for both LT and HT technologies is how integration with existing chemical clusters can be arranged. Specific use cases may result in more efficient integration of a technology into an industrial system. This may also involve specific locations or connections with renewable electricity sources like wind parks or large scale solar plants.

6 Conclusions

This review and analysis shows that several electrochemical technologies are available to convert CO_2 into different products. All routes are currently significantly more expensive in comparison with fossil-based approaches, but stringent climate

targets in combination with technology development may in the future favour renewable alternative approaches. The chlor-alkali process, as an example of a mature electrochemical process, can function as a starting point for reference and potential technology developments, especially for LT technology. The LT routes seem to be mainly based on membrane-type electrolyser systems and can benefit from developments in water electrolysis and fuel cell applications, *e.g.* PEM technology. HT systems are less comparable to membrane technology and are better compared with solid state fuel cell technology, such as SOFC and MCFC. Solid oxide technology seems most advanced in technology readiness and applied in larger scale CO_2 electroconversion demonstrators. These HT systems operate at a relatively high power density, which is comparable to HT steam electrolysis. The investment costs per unit output of HT systems are significantly lower than those of their LT counterparts.

Besides this current advantage in investment costs, the projected costs also reduce faster for the HT CO_2 conversion routes. This is mainly because in our learning curve analysis the assumed LR, which is based on solid oxide fuel cell technology, is slightly higher compared to LT technology for which the LR is based on LT water electrolysis, and the initial cumulative installed capacity of HT technology is relatively low, which makes relative capacity additions more likely to occur faster. The economic performance of all routes is mainly determined by the CAPEX component and thanks to steep learning of the HT pathways, these routes are likely first to reach break-even levelized production cost in comparison to the fossil reference. LT electrolysis processes still need a substantial reduction in investment costs to achieve break-even.

All electrochemical production routes to produce CO, formic acid, and syngas avoid or can soon avoid CO_2 emissions when compared to fossil reference processes. CO_2 taxation can therefore play a substantial role in the competitivity of electrochemical CO_2 conversion routes. In our base case projections, we find that for CO, formic acid, and syngas production, CO_2 taxation should range between at least 60 and 636€ per t_{CO_2} to break even with the fossil reference price. The most promising to reach break-even costs are LT formic acid production (CO_2 tax of 72€ per t_{CO_2}) and HT CO production (CO_2 tax of 60€ per t_{CO_2}). A higher CO_2 penalty would be required if the electricity that is used in the electroconversion routes is accompanied by an emission factor greater than zero. For ethylene production, saving GHG emissions by the electrochemical routes (3 and 6) becomes difficult if the efficiency and power density cannot be substantially improved without raising the investment costs. Our projections indicate that only with a CO_2 taxation of more than 2000€ per t_{CO_2} these routes may become competitive with the current fossil-based benchmark, which is not realistically feasible.

The early development stage of the investigated technologies also proffers opportunity for improvements and innovation that can drastically increase the technological performance. Research gaps are identified at various levels: materials, catalysts, electrodes, lifetime and associated maintenance costs of the active materials. Purification of both the feedstock and product, and downstream processing costs depend on the feedstock and product requirements. The early-stage research often does not focus on these up- and downstream processes and further study is necessary. Pilot projects demonstrating the entire product chain, from the industrial or atmospheric CO_2 source to the final product, can aid in the accurate assessment of the performance, total investment costs, and operating and maintenance costs in an industrial environment. More development and investments are deemed necessary to ensure technological learning effects and cost reductions of electrochemical CO_2 conversion routes. An advantage of these specific processes is that they can benefit from experience obtained in comparable technologies, such as water electrolysers and fuel cells.

Author contributions

RJD, AJK, and JK: conceptualization. RJD and AJK: methodology. RJD, CJF, CSM, MS, and MVS: investigation and analysis. RJD, CJF, AJK, CSM, and MVS: writing—original draft. RJD: produced final manuscript. RJD, CJF, AJK, JK, CSM, MS, and MVS: discussed and reviewed the results. RJD, CJF, CSM, and MVS: visualization. AJK and JK: project management and acquisition. All authors contributed to the article and approved the submitted version.

Conflicts of interest

There are no conflicts to declare.

Acknowledgements

The authors acknowledge T. Manders, G. J. Kramer, and S. Krishnan for stimulating discussions that helped improve the quality of our study. We acknowledge the IEA Greenhouse Gas R&D Programme for the funding of this project.

References

1 P. Friedlingstein, M. W. Jones, M. O'Sullivan, R. M. Andrew, D. C. E. Bakker, J. Hauck, C. Le Quéré, G. P. Peters, W. Peters, J. Pongratz, S. Sitch, J. G. Canadell, P. Ciais, R. B. Jackson, S. R. Alin, P. Anthoni, N. R. Bates, M. Becker, N. Bellouin, L. Bopp, T. T. T. Chau, F. Chevallier, L. P. Chini, M. Cronin, K. I. Currie, B. Decharme, L. Djeutchouang, X. Dou, W. Evans, R. A. Feely, L. Feng, T. Gasser, D. Gilfillan, T. Gkritzalis, G. Grassi, L. Gregor, N. Gruber, Ö. Gürses, I. Harris, R. A. Houghton, G. C. Hurtt, Y. Iida, T. Ilyina, I. T. Luijkx, A. K. Jain, S. D. Jones, E. Kato, D. Kennedy, K. Klein Goldewijk, J. Knauer, J. I. Korsbakken, A. Körtzinger, P. Landschützer, S. K. Lauvset, N. Lefèvre, S. Lienert, J. Liu, G. Marland, P. C. McGuire, J. R. Melton, D. R. Munro, J. E. M. S. Nabel, S.-I. Nakaoka, Y. Niwa, T. Ono, D. Pierrot, B. Poulter, G. Rehder, L. Resplandy, E. Robertson, C. Rödenbeck, T. M. Rosan, J. Schwinger, C. Schwingshackl, R. Séférian, A. J. Sutton, C. Sweeney, T. Tanhua, P. P. Tans, H. Tian, B. Tilbrook, F. Tubiello,

G. van der Werf, C. Wada, R. Wanninkhof, A. Watson, D. Willis, A. J. Wiltshire, W. Yuan, C. Yue, X. Yue, S. Zaehle and J. Zeng, Earth System Science Data Discussion [preprint], *Global Carbon Budget*, 2021, DOI: 10.5194/essd-2021-386.

2 R. J. Detz and B. van der Zwaan, *Energy Policy*, 2019, **133**, 110938, DOI: 10.1016/j.enpol.2019.110938.

3 IEAGHG, *CO_2 as a Feedstock: Comparison of CCU Pathways*, IEAGHG Technical Report, 2021-02, 2021, Retrieved from: https://www.ieaghg.org/.

4 International Energy Agency (IEA), *Putting CO_2 to use. Creating value from emissions*, 2019, Retrieved from: https://www.iea.org.

5 International Energy Agency (IEA), *Energy Technology Perspectives 2020. Special Report on Carbon Capture, Utilisation and Storage*, 2020, Retrieved from: https://www.iea.org.

6 Y. Jiang, M. Su, Y. Zhang, G. Zhan, Y. Tao and D. Li, *Int. J. Hydrogen Energy*, 2013, **38**, 3497–3502.

7 C. Li, T. Wang, B. Liu, M. Chen, A. Li, G. Zhang, M. Du, H. Wang, S. F. Liu and J. Gong, *Energy Environ. Sci.*, 2019, **12**, 923–928, DOI: 10.1039/C8EE02768D.

8 S.-F. Ng, J. Jie Foo and W.-J. Ong, *InfoMat*, 2022, **4**(1), e12279.

9 IEAGHG, *CO2 Utilisation: Hydrogenation Pathways*, IEAGHG Technical Report, 2021-03, 2021, Retrieved from: https://www.ieaghg.org/.

10 S. Lu, Y. Shi, N. Meng, S. Lu, Y. Yu and B. Zhang, *Cell Rep. Phys. Sci.*, 2020, **1**(11), 100237.

11 A. Sedighian Rasouli, X. Wang, J. Wicks, G. Lee, T. Peng, F. Li, C. McCallum, C.-T. Dinh, A. H. Ip, D. Sinton and E. H. Sargent, *ACS Sustainable Chem. Eng.*, 2020, **8**(39), 14668–14673.

12 J. Albo, A. Sáez, J. Solla-Gullón, V. Montiel and A. Irabien, *Appl. Catal., B*, 2015, **176–177**, 709–717, DOI: 10.1016/j.apcatb.2015.04.055.

13 K. Nakata, T. Ozaki, C. Terashima, A. Fujishima and Y. Einaga, *Angew. Chem., Int. Ed.*, 2014, **53**(3), 871–874, DOI: 10.1002/anie.201308657.

14 M. König, S.-H. Lin, J. Vaes, D. Pant and E. Klemm, *Faraday Discuss.*, 2021, **230**, 360–374, DOI: 10.1039/D0FD00141D.

15 D. Karapinar, C. E. Creissen, J. Guillermo Rivera de la Cruz, M. W. Schreiber and M. Fontecave, *ACS Energy Lett.*, 2021, **6**(2), 694–706.

16 X. Wang, P. Ou, A. Ozden, *et al.*, *Nat. Energy*, 2022, **7**, 170–176, DOI: 10.1038/s41560-021-00967-7.

17 T. F. O'Brien, T. V. Bommaraju and F. Hine, *Handbook of Chlor-Alkali Technology*, Springer, New York, 2005, vol. 1.

18 J. Crook and A. Mousavi, *Environ. Forensics*, 2016, **17**(3), 211–217, DOI: 10.1080/15275922.2016.1177755.

19 T. Brinkmann, G. Giner Santonja, F. Schorcht, S. Roudier and L. Delgado Sancho, *Best Available Techniques Reference Document for the Production of Chlor-Alkali*, 2014, DOI: 10.2791/13138.

20 Eurochlor, *Personal Communication with Ton Manders (on 29-04-2022)*, 2022.

21 Thyssenkrupp, *Chlor-Alkali Solutions*, 2022, Retrieved from: https://thyssenkrupp-nucera.com/chlor-alkali-solutions/.

22 Eurochlor, *The Electrolysis process and the real costs of production*, 2018, Retrieved from: https://www.eurochlor.org/wp-content/uploads/2019/04/12-electrolysis_production_costs.pdf.

23 International Energy Agency (IEA), *The Future of Hydrogen. Seizing today's opportunities*, 2019, Retrieved from: https://www.iea.org.

24 Thyssenkrupp, *Chlor-Alkali electrolysis plants. Superior membrane process*, 2015, Retrieved from: https://www.thyssenkrupp-industrial-solutions-rus.com/assets/pdf/TKIS_Chlor-Alkali_Electrolysis.pdf.

25 T. Smolinka, N. Wiebe, P. Sterchele, A. Palzer, F. Lehner, M. Jansen, S. Kiemel, R. Miehe, S. Wahren and F. Zimmermann, *Studie IndWEDe, Industrialisierung der Wasserelektrolyse in Deutschland: Chancen und Herausforderungen für nachhaltigen Wasserstoff für Verkehr*, Nationale Organisation Wasserstoff- und Brennstoffzellentechnologie – NOW GmbH, Strom und Wärme, 2018.

26 International Renewable Energy Agency (IRENA), *Green Hydrogen Cost Reduction: Scaling up Electrolysers to Meet the 1.5 °C Climate Goal*, International Renewable Energy Agency, Abu Dhabi, 2020, Retrieved from: https://www.irena.org/.

27 International Energy Agency (IEA), *Net Zero by 2050 - A Roadmap for the Global Energy Sector*, 2021, Retrieved from: https://www.iea.org.

28 J. K. Nørskov, A. Latimer and C. F. Dickens, *Research needs towards sustainable production of fuels and chemicals*, 2019, Retrieved from: https://www.energy-x.eu/research-needs-report/.

29 Siemens, *Rheticus: World's-first-automated-CO2-electrolyzer, Siemens Energy Global*, 2020, Retrieved from: https://www.siemens-energy.com.

30 R. Küngas, *J. Electrochem. Soc.*, 2020, **167**(4), 044508, DOI: 10.1149/1945-7111/ab7099.

31 K. Yang, M. Li, S. Subramanian, M. A. Blommaert, W. A. Smith and T. Burdyny, *ACS Energy Lett.*, 2021, **6**(12), 4291–4298, DOI: 10.1021/acsenergylett.1c02058.

32 D. W. Keith, G. Holmes, D. S. Angelo and K. Heidel, *Joule*, 2018, **2**(8), 1573–1594, DOI: 10.1016/j.joule.2018.05.006.

33 *Air Products*, 2022, Retrieved from: https://www.airproducts.com/-/media/airproducts/files/en/900/900-13-100-us-carbon-monoxide-safetygram-19.pdf.

34 Z. Liu, H. Yang, R. Kutz and R. I. Masel, *J. Electrochem. Soc.*, 2018, **165**(15), J3371–J3377, DOI: 10.1149/2.0501815jes.

35 R. Tichler, H. Böhm, A. Zauner, S. Goers, P. Kroon and S. Schirrmeister, *Innovative large-scale energy storage technologies and Power-to-Gas concepts after optimization. Report on experience curves and economies of scale*, 2018, Retrieved from: https://www.storeandgo.info/fileadmin/downloads/deliverables_2019/20190801-STOREandGO-D7.5-EIL-Report_on_experience_curves_and_economies_of_scale.pdf.

36 M. Jouny, W. Luc and F. Jiao, *Ind. Eng. Chem. Res.*, 2018, **57**(6), 2165–2177, DOI: **10.1021/acs.iecr.7b03514**.
37 A. Paturska, M. Repele and G. Bazbauers, *Energy Procedia*, 2015, **72**, 71–78, DOI: **10.1016/j.egypro.2015.06.011**.
38 A. Patonia and R. Poudineh, *Cost-competitive green hydrogen: how to lower the cost of electrolysers?*, 2022, Retrieved from: **https://www.oxfordenergy.org/**.
39 H. Böhm, S. Goers and A. Zauner, *Int. J. Hydrogen Energy*, 2019, **44**(59), 30789–30805, DOI: **10.1016/j.ijhydene.2019.09.230**.
40 A. Mayyas, M. Ruth, B. Pivovar, G. Bender and K. Wipke, *Manufacturing Cost Analysis for Proton Exchange Membrane Water Electrolyzers*, 2019, **https://doi.org/NREL/TP-6A20-72740**.
41 E. Schuler, M. Demetriou, N. R. Shiju and G. J. M. Gruter, *ChemSusChem*, 2021, **14**(18), 3636–3664, DOI: **10.1002/cssc.202101272**.
42 M. Ramdin, A. R. T. Morrison, M. De Groen, R. van Haperen, R. De Kler, E. Irtem, A. T. Laitinen, L. J. P. van den Broeke, T. Breugelmans, J. P. M. Trusler, W. de Jong and T. J. H. Vlugt, *Ind. Eng. Chem. Res.*, 2019, **58**(51), 22718–22740, DOI: **10.1021/acs.iecr.9b03970**.
43 OCEAN, *Oxalic acid from CO_2 using Electrochemistry At demonstratioN scale|SPIRE*, 2022, Retrieved from: **https://aspire2050.eu**.
44 E2c, *Electrons to high value Chemical products|2 Mers Seas Zeeën*, 2022, Retrieved from: **https://interreg2seas.eu**.
45 Q. Zhu, *Clean Energy*, 2019, **3**(2), 85–100, DOI: **10.1093/ce/zkz008**.
46 H. Yang, J. J. Kaczur, S. D. Sajjad and R. I. Masel, *J. CO2 Util.*, 2017, **20**, 208–217, DOI: **10.1016/j.jcou.2017.04.011**.
47 H. Yang, J. J. Kaczur, S. D. Sajjad and R. I. Masel, *J. CO2 Util.*, 2020, **42**, 101349, DOI: **10.1016/j.jcou.2020.101349**.
48 *SELECT CO_2*, 2022, Retrieved from: **https://selectco2.eu**.
49 *Energiforskning*, 2022, Retrieved from: **https://energiforskning.dk/projekter/electrochemical-co2-reduction-to-ethylene-industrial-applications**.
50 C. M. Gabardo, C. P. O'Brien, J. P. Edwards, C. McCallum, Y. Xu, C. T. Dinh, J. Li, E. H. Sargent and D. Sinton, *Joule*, 2019, **3**(11), 2777–2791, DOI: **10.1016/j.joule.2019.07.021**.
51 J. Sisler, S. Khan, A. H. Ip, M. W. Schreiber, S. A. Jaffer, E. R. Bobicki, C. T. Dinh and E. H. Sargent, *ACS Energy Lett.*, 2021, **6**(3), 997–1002, DOI: **10.1021/acsenergylett.0c02633**.
52 NIH, 2022, Retrieved from: **https://Ethylene-Some-Industrial-Chemicals-NCBI-Bookshelf-(nih.gov)**.
53 X. Wang, J. Ferreira de Araújo, W. Ju, A. Bagger, H. Schmies, S. Kühl, J. Rossmeisl and P. Strasser, *Nat. Nanotechnol.*, 2019, **14**, 1063–1070.
54 C. T. Dinh, T. Burdyny, G. Kibria, A. Seifitokaldani, C. M. Gabardo, F. P. G. de Arquer, A. Kiani, J. P. Edwards, P. De Luna, O. S. Bushuyev, C. Zou, R. Quintero-Bermudez, Y. Pang, D. Sinton and E. H. Sargent, *Science*, 2018, **787**, 783–787.
55 A. Hauch, R. Küngas, P. Blennow, A. B. Hansen, J. B. Hansen, B. V. Mathiesen and M. B. Mogensen, *Science*, 2020, **370**(186), eaba6118, DOI: **10.1126/science.aba6118**.
56 S. C. Singhal, *WIREs Energy and Environment*, 2014, **3**(2), 179–194, DOI: **10.1002/wene.96**.
57 J. D. Duhn, *Development of Highly Efficient Solid Oxide Electrolyzer Cell Systems*. Technical University of Denmark, 2017, Retrieved from: **https://orbit.dtu.dk/en/publications/development-of-highly-efficient-solid-oxide-electrolyzer-cell-sys**.
58 R. Küngas, P. Blennow, T. Heiredal-Clausen, T. Holt Nørby, J. Rass-Hansen, J. B. Hansen and P. G. Moses, *ECS Trans.*, 2019, **91**, 215.
59 F. Kasuya and T. Tsuji, *Gas Sep. Purif.*, 1991, **5**(4), 242–246.
60 S. Foit, L. Dittrich, T. Duyster, I. Vinke, R. Eichel and L. de Haart, *Processes*, 2020, **8**(11), 1390.
61 Hydrogen Europe, *Strategic Research and Innovation Agenda*, 2020, Retrieved from: **https://www.clean-hydrogen.europa.eu/about-us/key-documents/strategic-research-and-innovation-agenda_en**.
62 European Commission, *Communication from the Commission to the European Parliament, the Council, the European Economic and Social Committee and the Committee of the Regions*, 2020.
63 NewSoc, *Next Generation of Solid Oxide Fuel Cell and Electrolysis Technology*, 2022, Retrieved from: **https://Home-NewSoc-English**.
64 Clean Hydrogen Joint Undertaking (CHJU), *Strategic Research and Innovation Agenda 2021 – 2027*, 2021, p. 153.
65 Ulrik Frøhlke, *Haldor Topsoe to build large-scale SOEC electrolyzer manufacturing facility to meet customer needs for green hydrogen production*, 2021, Retrieved from: **https://blog.topsoe.com/haldor-topsoe-to-build-large-scale-soec-electrolyzer-manufacturing-facility-to-meet-customer-needs-for-green-hydrogen-production**.
66 M. Riegraf, D.-M. Amaya-Duenas, A. Surrey and R. Costa, *Evaluation of the Stability of Ni/CGO-Based Electrolyte Supported Cells in Co-electrolysis*, 12th European SOFC & SOE Forum, B0504, 2016.
67 A. Hauch, M. L. Traulsen, R. Küngas and T. L. Skafte, *J. Power Sources*, 2021, **506**, 230108.
68 *Sunfire*, 2021, Retrieved from: **https://www.sunfire.de/files/sunfire/images/content/Produkte_Technologie/factsheets/Sunfire-SynLink_FactSheet.pdf**.
69 A. Masini, T. Strohbach, F. Siska, Z. Chlup and I. Slouhy, *Materials*, 2019, **12**, 306.
70 *Sunfire*, 2022, Retrieved from: **https://webflow.com**.
71 *Sunfire*, 2022, Retrieved from: **https://SynLink**.
72 *Eco*, 2019, Retrieved from: **https://eco-soec-project**.
73 *Kopernikus*, 2019, Retreived from: **https://Kopernikus-Projekte:Kopernikus-Project:P2X**.
74 *N. e-fuel*, 2022, Retrieved from: **https://norsk-e-fuel.com**.
75 *MegaSyn*, 2022, Retreived from: **https://www.fch.europa.eu**.
76 F. P. F. van Berkel, C. J. Ferchaud, O. Partenie, M. J. G. Linders and Y. C. van Delft, *ECS Trans.*, 2021, **103**(1), 591–602.
77 O. Posdziech, *Production of Renewable Hydrogen and Syngas via High-Temperature Electrolysis, Presentation Sunfire on*

Heat-To-Fuel Interfaces to Advanced Power-To-Gas and Power-To-Liquids Technologies, 2021, **https://e-fuels**.
78 L. Hu, *Molten Carbonate Fuel Cells for Electrolysis*, Doctoral Thesis of KTH Royal Institute of Technology, 2016, ISSN 1654-1081, ISBN 978-91-7595-928-3.
79 Fuel Cell Energy, *MCFC system product data sheet*, 2022, Retreived from: **https://www.fuelcellenergy.com/**.
80 POSCO, *POSCO Energy Website – Fuel Cell Development*, 2022, Retreived from: **https://posco-energy-Products**.
81 R. Bove, A. Moreno and S. McPhail, *International Status of Molten Carbonate Fuel Cell (MCFC) Technology*, EUR 23363 EN, European Commission JRC44203, Luxembourg (Luxembourg), 2008.
82 M. Jouny, W. Luc and F. Jiao, *Nat. Catal.*, 2018, **1**(10), 748–755, DOI: **10.1038/s41929-018-0133-2**.
83 M. Jouny, G. S. Hutchings and F. Jiao, *Nat. Catal.*, 2019, **2**(12), 1062–1070, DOI: **10.1038/s41929-019-0388-2**.
84 D. S. Ripatti, T. R. Veltman and M. W. Kanan, *Joule*, 2019, **3**(1), 240–256, DOI: **10.1016/j.joule.2018.10.007**.
85 H. J. Lang, *Chem. Eng.*, 1948, **55**, 112.
86 Y. A. Wain, *PM World J.*, 2014, **3**, 10.
87 Hydrohub Innovation Program, *A One-GigaWatt Green-Hydrogen Plant. Advanced Design and Total Installed-Capital Costs*, 2022, Retrieved from: **https://ispt.eu/news/new-report-gigawatt-green-hydrogen-plant-advanced-design-and-total-installed-capital-costs/**.
88 G. Glenk and S. Reichelstein, *Nat. Energy*, 2019, **4**, 216–222.
89 R. Detz and M. Weeda, *Projections of Electrolyzer Investment Cost Reduction through Learning Curve Analysis*, TNO 2022 P10111, 2022, Retrieved from: **https://energy.nl/wp-content/uploads/tno-2022-p10111_detzweeda_projections-of-electrolyzer-investment-cost-reduction-through-learning-curve-analysis.pdf**.
90 R. J. Detz, J. N. H. Reek and B. C. C. van der Zwaan, *Energy Environ. Sci.*, 2018, **11**(7), 1653–1669.
91 J. Nyári, M. Magdeldin, M. Larmi, M. Järvinen and A. Santasalo-Aarnio, *J. CO2 Util.*, 2020, **39**, 101166, DOI: **10.1016/j.jcou.2020.101166**.
92 R. J. Detz and B. van der Zwaan, *J. Energy Chem.*, 2022, **71**, 507–513.
93 *Methanex*, 2022, Retreived from: **https://Pricing|Methanex-Corporation**.
94 *ChemAnalist*, 2022, Retrieved from: **https://Formic-Acid-Prices-Price-Pricing-News|ChemAnalyst**.
95 *ChemAnalist*, 2022, Retrieved from: **https://Ethylene-Prices-News-Market-Analysis|ChemAnalyst**.
96 A. McDonald and L. Schrattenholzer, *Energy Policy*, 2001, **29**, 255–261.
97 F. Ferioli, K. Schoots and B. C. C. van der Zwaan, *Energy Policy*, 2009, **37**, 2525–2535.
98 *International Technology Roadmap for Photovoltaic (ITRPV)*, 2022, Retrieved from: **https://www.vdma.org/international-technology-roadmap-photovoltaic**.
99 E. S. Rubin, I. M. L. Azevedo, P. Jaramillo and S. Yeh, *Energy Policy*, 2015, **86**, 198–218.
100 K. Schoots, F. Ferioli, G. J. Kramer and B. C. C. van der Zwaan, *Int. J. Hydrogen Energy*, 2008, **33**, 2630–2645.
101 O. Schmidt, A. Hawkes, A. Gambhir and I. Staffell, *Nat. Energy*, 2017, **2**, 17110.
102 S. Krishnan, M. Fairlie, P. Andres, T. de Groot and G. J. Kramer, Technological Learning in the Transition to a Low-Carbon Energy System, Conceptual Issues, Empirical Findings, and Use in Energy Modeling, *Chapter 10: Power to gas (H2): alkaline electrolysis*, 2020, pp. 165–187.
103 K. Schoots, G. J. Kramer and B. C. C. van der Zwaan, *Energy Policy*, 2010, **38**, 2887–2897.
104 M. Wei, S. J. Smith and M. D. Sohn, *App. Energy*, 2017, **191**, 346–357.
105 Global Wind Energy Council, *Global Wind Report 2022*, 2022, Retrieved from: **https://gwec.net/global-wind-report-2022/**.
106 R. Rivera-Tinoco, K. Schoots and B. C. C. van der Zwaan, *Energy Convers. Manage.*, 2012, **57**, 86–96.
107 G. J. van Rooij, H. N. Akse, W. A. Bongers and M. C. M. van de Sanden, *Plasma Phys. Controlled Fusion*, 2018, **60**, 014–019.
108 International Energy Agency (IEA), *20 Years of Carbon Capture and Storage, Accelerating Future Deployment*, 2016, Retrieved from: **https://www.iea.org**.
109 L. Irlam, *Global CCS Institute, Global costs of carbon capture and storage*, 2017, Retrieved from: **https://www.globalccsinstitute.com/**.
110 M. Fasihi, O. Efimova and C. Breyer, *J. Cleaner Prod.*, 2019, **224**, 957e980, DOI: **10.1016/j.jclepro.2019.03.086**.
111 Renewable Energy Directive II, *Directive (EU) 2018/2001 of the European Parliament and of the Council of 11 December 2018 on the promotion of the use of energy from renewable sources*, Official Journal of the European Union, 2018.
112 I. E. L. Stephens, K. Chan, A. Bagger, S. W. Boettcher, J. Bonin, E. Boutin, A. Buckley, R. Buonsanti, E. Cave, X. Chang, S. W. Chee, A. H. M. da Silva, P. De Luna, O. Einsle, B. Endrődi, M. Escudero-Escribano, J. V. F. de Araujo, M. C. Figueiredo, C. Hahn and Y. Zhou, *Mater. Today: Proc.*, 2019, **27**, 0–31, DOI: **10.1088/2515-7655/ac7823**.
113 J. J. Kaczur, L. J. McGlaughlin and P. S. Lakkaraju, *C*, 2020, **6**(2), 42, DOI: **10.3390/c6020042**.
114 M. G. Kibria, J. P. Edwards, C. M. Gabardo, C. T. Dinh, A. Seifitokaldani, D. Sinton and E. H. Sargent, *Adv. Mater.*, 2019, **31**(31), 1–24, DOI: **10.1002/adma.201807166**.
115 D. Reinisch, B. Schmid, N. Martić, R. Krause, H. Landes, M. Hanebuth, K. J. J. Mayrhofer and G. Schmid, *Z. Fur Phys. Chem.*, 2020, **234**(6), 1115–1131, DOI: **10.1515/zpch-2019-1480**.
116 J. Y. "Timothy" Kim, P. Zhu, F.-Y. Chen, Z.-Y. Wu, D. A. Cullen and H. Wang, *Nat. Catal.*, 2022, **5**, 288–299, DOI: **10.1038/s41929-022-00763-w**.
117 K. Xie, A. Ozden, R. K. Miao and E. H. Sargent, *Nat. Commun.*, 2022, **13**(3070), 1–9, DOI: **10.1038/s41467-022-30677-x**.
118 J. Pérez-Carbajo, I. Matito-Martos, S. R. G. Balestra, M. N. Tsampas, M. C. M. van de Sanden, J. A. Delgado, V. I. Águeda, P. J. Merkling and S. Calero, *ACS Appl.*

Mater. Interfaces, 2018, **10**(24), 20512–20520, DOI: **10.1021/acsami.8b04507**.

119 S. Samipour, M. D. Manshadi and P. Setoodeh, *ACS Appl. Mater. Interfaces*, 2020, **1**, 455–477, DOI: **10.1016/b978-0-12-819657-1.00020-7**.

120 Á. Vass, A. Kormányos, Z. Kószó, B. Endrődi and C. Janáky, *ACS Catal.*, 2022, **12**(2), 1037–1051, DOI: **10.1021/acscatal.1c04978**.

121 J. Jack, W. Zhu, J. L. Avalos, J. Gong and Z. J. Ren, *Green Chem.*, 2021, **23**(20), 7917–7936, DOI: **10.1039/d1gc02094c**.

122 E. Pérez-Gallent, S. Turk, R. Latsuzbaia, R. Bhardwaj, A. Anastasopol, F. Sastre-Calabuig, A. C. Garcia, E. Giling and E. L. V. Goetheer, *Ind. Eng. Chem. Res.*, 2019, **58**(16), 6195–6202.

123 Á. Vass, B. Endrődi and C. Janáky, *Curr. Opin. Electrochem.*, 2021, **25**, 1–9, DOI: **10.1016/j.coelec.2020.08.003**.

124 T. E. Lister and E. J. Dufek, *Energy Fuels*, 2013, **27**(8), 4244–4249, DOI: **10.1021/ef302033j**.

125 S. Verma, S. Lu and P. J. A. Kenis, *Nat. Energy*, 2019, **4**, 466–474, DOI: **10.1038/s41560-019-0374-6**.

126 H. Shin, K. U. Hansen and F. Jiao, *Nat Sustainability*, 2021, **4**, 911–919, DOI: **10.1038/s41893-021-00739-x**.

127 *FCH*, 2022, More information can be find at: **https://www.fch.europa.eu**.

128 G. Min, Y. Park and J. Hong, *Energy Convers. Manage.*, 2020, **225**, 113381.

129 A. J. Martín, G. O. Larrazábal and J. Pérez-Ramírez, *Green Chem.*, 2015, **17**(12), 5114–5130, DOI: **10.1039/c5gc01893e**.

130 B. H. Ko, B. Hasa, H. Shin, E. Jeng, S. Overa, W. Chen and F. Jiao, *Nat. Commun.*, 2020, **11**(1), 1–9, DOI: **10.1038/s41467-020-19731-8**.

131 S. Overa, B. H. Ko, Y. Zhao and F. Jiao, *Acc. Chem. Res.*, 2022, **55**(5), 638–648, DOI: **10.1021/acs.accounts.1c00674**.

